



Impact of the altitude on the wood anatomical traits of *Calluna vulgaris*

Inês Boal Afonso de Oliveira Costa

Dissertation for Master's degree in
Management and Conservation of Natural Resources

Advisors: Cristina Nabais, University of Coimbra

Maria da Conceição Caldeira, University of Lisboa

Jury:

President: Doctor Maria Teresa Marques Ferreira, Full Professor at the School of Agriculture at the University of Lisbon

Members: Doctor Cristina Maria Filipe Máguas da Silva Hanson, Associate Professor at the Faculty of Sciences from the University of Lisbon;

Doctor Maria Cristina Amaral Penas Nabais dos Santos, Assistant Professor with aggregation of the University of Coimbra, supervisor;

Doctor Raquel Lobo do Vale, Researcher at the School of Agriculture at the University of Lisbon

Instituto Superior de Agronomia

Universidade de Lisboa

Impact of the altitude on the wood anatomical traits of *Calluna vulgaris*

Inês Boal Afonso

Dissertação orientada pela Professora Doutora Cristina Nabais e Professora Doutora Maria da Conceição Caldeira no âmbito do Mestrado de Gestão e Conservação de Recursos Naturais, Instituto Superior de Agronomia, Universidade de Lisboa.

Trabalho realizado no âmbito do projeto de investigação “Estrela - Effect of global warming on the diversity and functioning of the alpine ecosystems of Serra da Estrela, a threatened mountain range in the transition area between temperate and Mediterranean climates” com referência PTDC/BIA-CBI/30215/2017 (CENTRO-01-0145-FEDER-030215), co-financiado pelo Fundo Europeu de Desenvolvimento Regional (FEDER), através do programa Portugal-2020 (PT2020), no âmbito do Programa Operacional Regional do Centro e pela FCT/MCTES através de fundos nacionais (PIDDAC). Este trabalho foi realizado na Unidade de I&D Centre for Functional Ecology – Science for People & the Planet (CFE), com a referência UIDB/04004/2020, com apoio financeiro da FCT/MCTES através de fundos nacionais (PIDDAC)



Acknowledgments

My first big thanks go to Cristina, Susana, Marta, Ana, and all the colleagues at Coimbra, their help was essential for my growth as a professional and as a person, and for that, I will be forever thankful.

A second thanks go to my family and friends. Your support in my journey is inspirational (even with the big distance gap) and without it, I could never go as far as I am going with my career. A special thanks to Olga (grandmother), mom, Floki (dog), and my girl Mafalda. Your knowledge and support were essential. I'm grateful every day for having you in my life. Thank you!

My last, but not least important thanks go to the person with the most contagious smile and happiness that I had the pleasure to meet and be part of their life. Even though you had a short journey, you will always be present in my life, mind, and heart. I know you will be always present to give our family strength for everything we need forward and for all of that and beyond, I thank you.

I dedicate this thesis to the most happy-contagious person I will ever know, my cousin Edgar Abreu.

May we meet again,

With most love and a big hug, your "Inesoca"

Abstract

Climate change scenarios for the Iberian Peninsula forecast an increase in temperature and a considerable decline in precipitation for all seasons. Heat waves, floods, and other extreme events can be expected to challenge the ability of several species to survive the new environmental trends. *Calluna vulgaris* (L.) Hull is a small to medium-sized evergreen woody shrub, with a large geographical distribution, being able to survive freeze conditions below -20°C in Mediterranean climates. Probably *C. vulgaris* presents a high genetic diversity and/or a high morphological and physiological plasticity, translated in a high degree of adjustment to different climatic conditions.

To understand if *C. vulgaris* has high morphological plasticity, woody stems were collected from populations located at different altitudes in Serra da Estrela. The altitudinal gradient was used as a proxy for changing temperature. Several wood anatomical traits were measured: shrub-ring width (SRW), average vessel area (AVA), and percentage of cell wall (PCW). SRW was correlated with the prevalent climatic conditions. SRW from all populations showed a negative correlation with the summer temperature. Populations from lower altitudes showed a positive correlation with the minimum temperature of January, while the populations from higher altitudes showed a positive correlation with precipitation from May to September. The SRW, AVA, and PCW from 2016 to 2020 showed no significant differences between the populations.

The measured wood anatomical traits showed no significant differences with altitude, indicating that they are highly conserved, independent of the climatic conditions, or have a limited value as an adaptive trait. However, growth response to climatic conditions was slightly different between low and high-altitude populations of *C. vulgaris*, indicating adjustments in the response to the prevalent climatic conditions. Besides these results, more studies are necessary to understand shrub growth dynamics and adaptive traits, especially under scenarios of climate change.

Key-words: Cell wall, Climate change; Dendrochronology; Shrub-ring width; Vessel area

Resumo

Os cenários de alterações climáticas para a Península Ibérica preveem um aumento da temperatura e uma diminuição considerável da precipitação para todas as estações. Um aumento da frequência das ondas de calor, inundações e outros eventos extremos vão desafiar a capacidade de várias espécies de sobreviver às novas tendências climáticas. *Calluna vulgaris* (L.) Hull é um arbusto lenhoso perene com ampla distribuição geográfica, sendo capaz de sobreviver a condições de congelamento abaixo de -20°C e em climas mediterrâneos. Provavelmente *C. vulgaris* apresenta uma alta diversidade genética e/ou alta plasticidade morfológica e fisiológica, traduzida num elevado grau de adaptação a diferentes condições climáticas.

Para compreender se *C. vulgaris* tem uma elevada plasticidade morfológica, foram recolhidos caules lenhosos de populações localizadas a diferentes altitudes na Serra da Estrela. O gradiente altitudinal foi usado como proxy de alteração da temperatura. Foram quantificados vários parâmetros anatómicos da madeira: largura do anel (SRW), área média dos vasos (AVA) e percentagem de parede celular (PCW). O SRW foi correlacionado com as condições climáticas. O SRW de todas as populações apresentou uma correlação negativa com a temperatura de verão. As populações de altitudes mais baixas apresentaram uma correlação positiva com a temperatura mínima de Janeiro, enquanto as populações de altitudes mais elevadas apresentaram uma correlação positiva com a precipitação de Maio a Setembro. O SRW, AVA e PCW de 2016 a 2020 não apresentaram diferenças significativas entre as populações.

As características anatómicas da madeira que foram quantificadas não apresentaram diferenças significativas com a altitude, indicando que são altamente conservadas, independentemente das condições climáticas, ou têm um valor limitado como característica adaptativa. No entanto, as populações indicaram um ajustamento na resposta às condições climáticas. Apesar destes resultados, mais estudos em arbustos serão necessários para entender sua dinâmica de crescimento e características adaptativas, especialmente em cenários de mudanças climáticas.

Palavras-chave: Parede celular; Alterações climáticas; Dendrocronologia; Tamanho do anel; Área dos vasos.

Resumo desenvolvido

Os cenários de alterações climáticas para a Península Ibérica preveem um aumento da temperatura e uma diminuição considerável da precipitação para todas as estações. Um aumento da frequência das ondas de calor, inundações e outros eventos extremos desafiam a capacidade de várias espécies de sobreviver às novas tendências climáticas. As áreas de montanha, tendo a temperatura como fator limitante para o crescimento das plantas, estão especialmente expostas ao impacto das alterações climáticas, prevendo-se uma subida em altitude de espécies de plantas que antes estavam limitadas pelo fator temperatura, colocando em causa o habitat de espécies adaptadas a temperaturas mais baixas. A Serra da Estrela, a cadeia montanhosa mais alta de Portugal Continental, situa-se na transição entre os bioclimas temperado e mediterrâneo, apresentando diferentes características ecológicas e climáticas ao longo de várias altitudes. É possível definir três níveis altitudinais na Serra da Estrela, cada um apresentando características climáticas e ecológicas distintas: o nível mais baixo que vai até aos 800 metros de altitude, o nível médio com altitudes entre os 800 e 1600 metros e, por último, o nível mais alto, com altitudes entre os 1600 e 1993 metros, sendo este o ponto mais alto da Serra da Estrela. Conforme a altitude e estação do ano, as temperaturas podem variar entre -10°C e 30°C. A Serra da Estrela representa uma área com especial interesse para a conservação da biodiversidade e para além disso, nesta montanha nascem dois dos maiores rios de Portugal, o rio Zêzere e o rio Mondego. Estudos alertam para uma alta possibilidade dos recursos hídricos na Serra da Estrela se tornarem mais vulneráveis tendo em conta os cenários das alterações climáticas de aumento da temperatura e diminuição da precipitação.

Calluna vulgaris (L.) Hull é um arbusto lenhoso perene de pequeno a médio porte, com ampla distribuição geográfica, sendo capaz de sobreviver a condições de congelamento abaixo de -20°C e em climas mediterrâneos. Provavelmente *C. vulgaris* apresenta uma alta diversidade genética e/ou alta plasticidade morfológica e fisiológica, traduzida num elevado grau de adaptação a diferentes condições climáticas. Para compreender se *C. vulgaris* tem uma elevada plasticidade morfológica, foram recolhidos caules lenhosos de *C. vulgaris* de populações localizadas a diferentes altitudes na Serra da Estrela. O gradiente altitudinal foi usado como proxy

de alteração da temperatura. Foram quantificados vários parâmetros anatómicos da madeira: largura do anel (SRW), área média dos vasos (AVA) e percentagem de parede celular (PCW). O SRW foi ainda correlacionado com as condições climáticas. Esperamos que as características anatómicas da madeira de *C. vulgaris* apresentem alta plasticidade, representando um alto grau de adaptação a diferentes condições climáticas. As principais hipóteses deste trabalho são:

- i. A largura do anel de crescimento diminui com a altitude porque a estação de crescimento é mais curta;
- ii. A área dos vasos diminui com a altitude, devido às temperaturas de congelamento, pois vasos maiores são mais suscetíveis à cavitação provocado pelos ciclos de congelamento/descongelamento da seiva;
- iii. A percentagem de parede celular aumenta com a altitude, aumentando a força mecânica para resistir ao vento e à cobertura de neve.

Selecionaram-se 3 níveis de altitude (250, 1630 e 1850m) e em cada nível, foram selecionadas três populações de *C. vulgaris*. Uma vez que não foram encontradas populações de *C. vulgaris* nas altitudes mais baixas próximo da Serra da Estrela, estas populações foram selecionadas próximo da região de Coimbra. Em cada local de amostragem foi registado a altura e o diâmetro máximo de cada indivíduo e caracterizou-se a vegetação circundante. Em cada população foram amostrados 6 indivíduos e em cada indivíduo, três ramos. No laboratório foram feitas amostragens do caule lenhoso dos vários ramos. Uma vez que o tamanho dos vasos aumenta do ápice para a base dos ramos, para uniformizar esta relação alométrica, as amostras foram feitas mantendo uma distância do ápice de 20cm. As amostras foram posteriormente processadas seguindo um protocolo de amostras histológicas. As preparações anatómicas foram posteriormente observadas ao microscópio óptico e foram obtidas imagens para posterior análise dos parâmetros anatómicos, utilizando o programa ImageJ. A partir das imagens mediu-se o tamanho dos anéis de crescimento (SRW) e para o período entre 2016 e 2020, quantificou-se, por anel de crescimento, a área do lúmen dos vasos, que foi utilizada para calcular a área média

dos vasos (AVA), e a percentagem de parede celular (PCW). Foram feitas correlações entre as condições climáticas e o SRW e, para ver o efeito da altitude nos parâmetros anatómicos de 2016 a 2020 foram utilizados modelos lineares mistos, utilizando a altitude como fator fixo, e o local de amostragem de cada população e o ano como fatores aleatórios. Uma vez que as populações das altitudes mais baixas eram muito mais jovens do que as populações das altitudes mais elevadas, foi necessário remover o efeito da idade do tamanho do anel de crescimento. Os indivíduos mais jovens apresentam anéis de crescimento de maior dimensão do que os indivíduos mais velhos, uma relação alométrica conhecida da ciência dendrocronológica. Para remover o efeito da idade do SRW fez-se uma regressão entre estes dois parâmetros e utilizaram-se os residuais da regressão nos modelos lineares mistos.

As correlações entre o clima e o crescimento foram ligeiramente diferentes entre os locais de baixa e alta altitude. Um sinal comum a todas as populações, independentemente da altitude, foi a correlação negativa com a temperatura do verão, o que é esperado num clima mediterrâneo. As populações de baixa altitude mostraram uma correlação positiva marginal com a temperatura mínima em Janeiro, indicando a possibilidade de um início mais precoce da estação de crescimento. As populações das altitudes mais elevadas apresentaram uma correlação positiva com a precipitação de Maio a Setembro, indicando que a disponibilidade hídrica na primavera e no verão é importante para o crescimento da madeira.

As características anatómicas da madeira SRW, AVA e PCW medidas de 2016 a 2020, não apresentaram diferenças significativas entre as populações das altitudes baixas, intermédia e alta. Este resultado indica que os parâmetros anatómicos que foram quantificados são altamente conservados, mesmo quando os arbustos são submetidos a diferentes condições ambientais. No entanto, parece que as populações dos locais de maior altitude tendem a ter uma percentagem maior de vasos mais largos. A presença de vasos mais largos pode ser vantajosa quando a estação de crescimento é mais curta, porque aumenta a capacidade de transporte de água, mesmo que aumente a suscetibilidade à cavitação.

O aumento da temperatura previsto nas projeções das alterações climáticas, terá provavelmente impactos na dinâmica de crescimento de *C. vulgaris*. Populações em altitudes mais altas provavelmente começarão a estação de crescimento mais cedo, pois são limitadas por temperaturas mais baixas, mas o stress hídrico no verão irá aumentar, diminuindo o crescimento da madeira em populações de urze de baixa e alta altitude. Se vasos mais largos são uma característica adaptativa de populações de alta altitude a uma estação de crescimento mais curta, sob um cenário de aumento de stress hídrico, a presença de vasos mais largos pode aumentar a suscetibilidade à cavitação.

Os arbustos são estruturas complexas em termos de crescimento, em comparação com as árvores, e com menos estudos sobre características anatómicas da madeira e dendrocronologia. No entanto, os arbustos são um grupo funcional muito importante e dominante nas áreas alpinas e mediterrânicas. Assim, mais estudos são necessários para entender sua dinâmica de crescimento e características adaptativas, especialmente em cenários de mudanças climáticas.

Contents

Acknowledgments	iv
Abstract	v
Resumo	vii
Resumo desenvolvido	ix
Abbreviation's list	xv
Introduction	1
Climate change in alpine ecosystems	1
Serra da Estrela: climate projections and potential impacts	4
<i>Calluna vulgaris</i> in Serra da Estrela	7
Wood anatomical traits of <i>C. vulgaris</i>	9
Objectives and hypothesis	12
Materials and methods	13
Study site and field sampling	13
Processing of wood samples	14
Image capture and analysis	17
Statistical analysis	19
<i>Climate-growth analysis</i>	19
<i>Wood traits and altitude</i>	20
Results	22
Age, height, and diameter of <i>C. vulgaris</i>	22
Climate-growth analysis	23
The effect of altitude on wood anatomical traits	25
Vessel area distribution frequency	29
Discussion	30
Age, height, and diameter of <i>C. vulgaris</i>	30
Growth series and climate correlations	31
Impact of altitude on SRW, AVA, and PCW	33

Conclusions	35
References	37
Appendix	47

Abbreviation's list

ALX - Lorigã

AVA - Average Vessels Area

CAM e BUR - Covão dos ponchos

CAR - Carapinheira da Serra

COB - Covão do Boi

CUM - Sabugueiro

EEA - European Environmental Agency

Eu - European Union

GHG – Greenhouse Gases

GLORIA - Global Observation Research Initiative in Alpine Environments

GMST – Global mean surface temperature

IP – Iberian Peninsula

IPA - IPARK de Coimbra

IPCC - Intergovernmental Panel on Climate Change

ISSG - Invasive Species Specialist Group

LAC - Lagoa comprida

LSAT - Land Surface Air Temperature

MIS – Misarela

SDMs - Species distribution models

SRW – Shrub Ring Width

PV - Vessels percentage

PCW – Cell Wall percentage

Introduction

Climate change in alpine ecosystems

In 2000, a group of geologists led by the Nobel Prize winner Paul Crutzen argue that human activity has altered the history of the earth so much that it become necessary to declare a new epoch to register this impact – The Anthropocene age (Trexler, 2015). The main impacts of this epoch are the increase in the human population and the associated increase in emissions of greenhouse gases (GHGs) (Trexler, 2015).

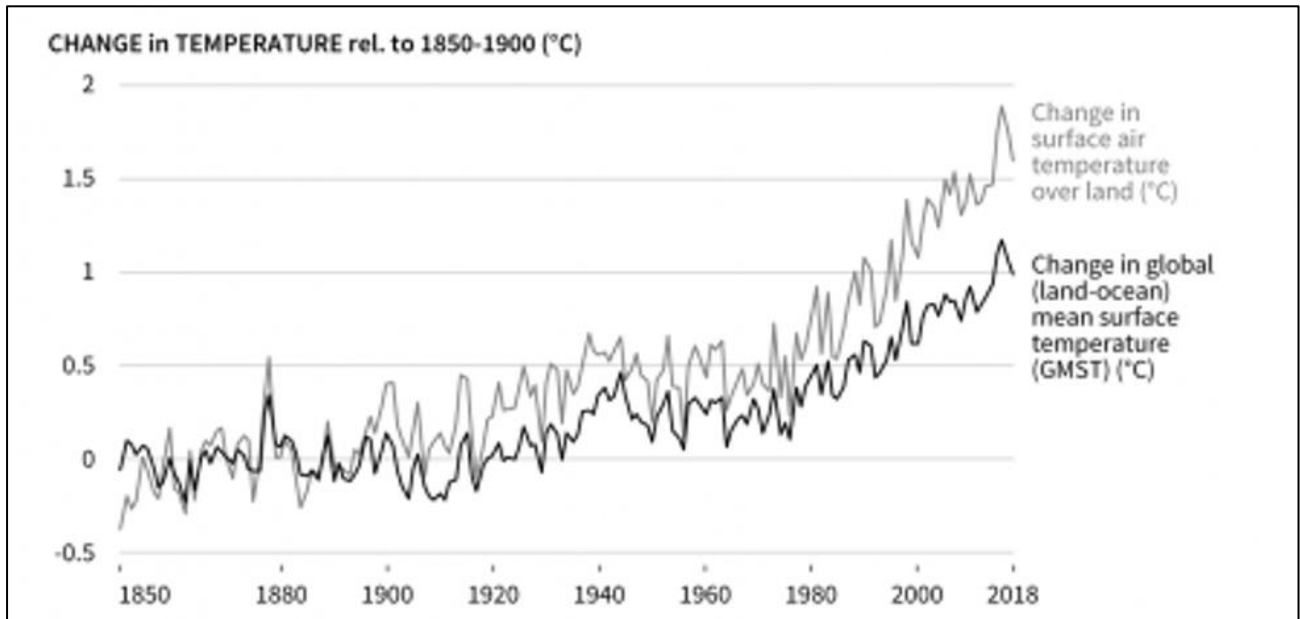


Figure 1 - Change in Land Surface Air Temperature (LSAT) and Global mean surface temperature (GMST), having as reference temperatures from the period 1850 – 1900 (Source: Jia et al., 2018)

Greenhouse gases exist in the atmosphere to absorb the heat excess that comes from the earth's surface, keeping the temperature balanced and possible for living beings to survive. But with the constant increase of the concentration in the atmosphere of GHGs, leads to an increase in temperature with impacts on the atmospheric circulation patterns (Martinez, 2005; Trexler, 2015). Reports of the Intergovernmental Panel on Climate Change (IPCC) show that the land surface air

temperature (LSAT) has risen faster than the global mean surface temperature (GMST - land, and ocean), having the preindustrial period (1850-1900) as a reference period, and showing an increase of 1.53°C (Jia *et al.*, 2018) (Figure 1). This warming resulted in climate shifts with an increase in dry climates, a higher frequency of extreme events, and the melting of the polar regions, shifting climate zones poleward, from mid to high latitudes, and upward, from lower to higher altitudes (Jia *et al.*, 2018). For the Iberian Peninsula (IP) temperature forecasts indicate a rising of about 2°C around the mid-21st century and up to 4°C by the end of the century (Pereira *et al.*, 2021). A reduction in the mean precipitation forecast for southern Europe, but at the same time, a higher frequency of days with heavy precipitation (Pereira *et al.*, 2021) gives major concerns around the IP region's vulnerability to dryness and floods.

With global warming, it is expected a higher frequency and intensity of droughts, heatwaves, fires, erosion, and a rising of the sea level, due to the melting of Greenland, which can lead to an increase in floods (Pereira *et al.*, 2021; Trexler, 2015). This will have important consequences on the ecosystems that will become increasingly exposed to impacts that can irreversibly change their structure, composition, and functioning. Climate change will affect the phenology of species, with consequences on species reproduction and establishment, distribution, and species interactions (Giménez-Benavides *et al.*, 2018; Winkler *et al.*, 2019; Alam, 2021; Skendžić *et al.*, 2021; Coelho *et al.*, 2021; Dahl *et al.*, 2021). According to Winkler *et al.*, 2019, inconsistent physiological and phenological responses to warming will depend on soil moisture, pollinator availability, and the ability of species to acclimate to changing conditions – also known as “plasticity”. A loss in biodiversity of 30% - 70% can be expected for the next 100 years (Román-Palacios & Wiens, 2020), which can cause an “extinction domino effect” and annihilate all life on earth (Strona & Bradshaw, 2018).

Alpine environments are ideal places to learn more about the ecological effect of climate change, as they provide temperature and ecological gradients, and above the tree line, there is a lower impact of human disturbance (Giménez-Benavides *et al.*, 2018). These ecosystems are very important not only because of their biodiversity richness but also because they act as seasonal

carbon sinks and water supply for many communities, including humans. Climate warming will cause a “cascade of interconnected responses that, as a whole, will alter alpine plant community composition and diversity”, as it is projected reduction of snow cover, with impacts on ground-level radiation regimes, soil microbial communities, and nutrient cycles (Winkler *et al.*, 2019). The increasing temperature will also have impacts on alpine plant species above the tree line, as subalpine species (trees included) are expected to expand upslope and establish in alpine habitats. Alpine areas are one of the most susceptible to species extinctions because species have less space for upward migration (Giménez-Benavides *et al.*, 2018). Alexander *et al.* (2018) and Malanson *et al.* (2019), modeled disequilibrium dynamics in alpine plant communities under future climate change based on tree line position, growth form, tree recruitment, or seedling establishment. Alexander *et al.* (2018) stated that “lags in species’ range responses to recent climate change along elevation gradients occur” and that “lags are common and likely to influence rates of community turnover in the future” – which has major implications for future structure and function of alpine communities. Additionally, biotic interactions will be crucial to mediate disequilibrium dynamics, and likely have a strong influence on establishment and extinction lags. These studies showed that it is important to understand the strategies used by specific species that can survive in different conditions along the altitude and are therefore less affected by extinction lags.

The alpine ecosystems located in Mediterranean climates have “remarkable levels of taxonomic diversity and singularity”, as reported by GLORIA (Global Observation Research Initiative in Alpine Environments), with a high percentage of plant endemism (Giménez-Benavides *et al.*, 2018). Species distribution models (SDMs) under projected climate change scenarios for the Mediterranean climate highlight that Mediterranean mountains are particularly sensitive to climate change and will become seriously affected in the future. Climate change in the Mediterranean is already having more impact on high-elevation habitats (Pugnaire *et al.*, 2021), and local-extinction events are highly correlated with high temperatures in most of the species studied (Román-Palacios & Wiens, 2020). Nonetheless, many species have genotypic and phenotypic plasticity, that can make them able to survive under extreme variations of environmental conditions.

However, more knowledge is needed to determine the most and less vulnerable species to climate change trends to prioritize biodiversity conservation measures.

Serra da Estrela: climate projections and potential impacts

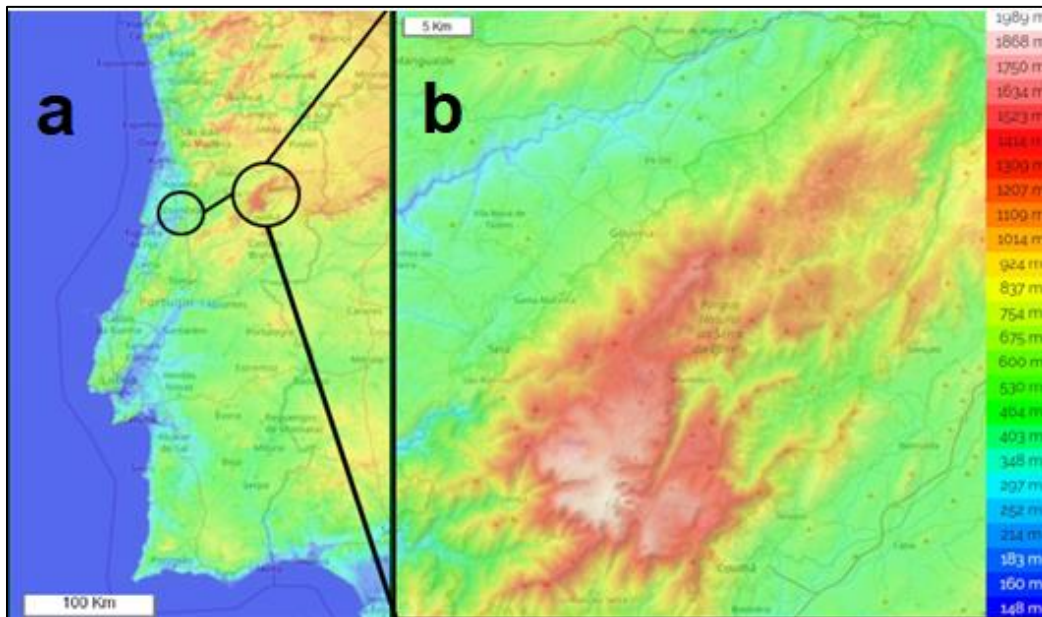


Figure 2 - Altitudinal map of Portugal (a) and Serra da Estrela (b). (Source: Topographic-map.com)

Serra da Estrela is part of the Iberian Central System, a mountain range that crosses the Iberian Peninsula, and is the highest mountain on Portugal's mainland, with 1993 meters (Figure 2). Since 1976 was classified as a Natural Park, and in 2020 was classified as part of the UNESCO Geopark. Different areas of this park have acquired different protection statuses from the European Union (EU): In 1993, a central part of the park was designated as a European biogenetic reserve. In 2000, a large part was included in Nature 2000, a network of sites that ensures the long-term survival of Europe's most valuable and threatened species and habitats. In 2003, was declared an important bird zone in Portugal. In 2005, the European Habitats Directive was

transposed to national law (Decreto-Lei 49/2005) and Serra da Estrela was designated as an internationally important humid zone under the Ramsar Convention (Jansen, 2011). According to European Environmental Agency, Serra da Estrela includes 37 species of the Nature Directives and 31 habitat types of the Habitats Directive (Appendix 1 and Appendix 2), reinforcing the importance of this park for conservation.

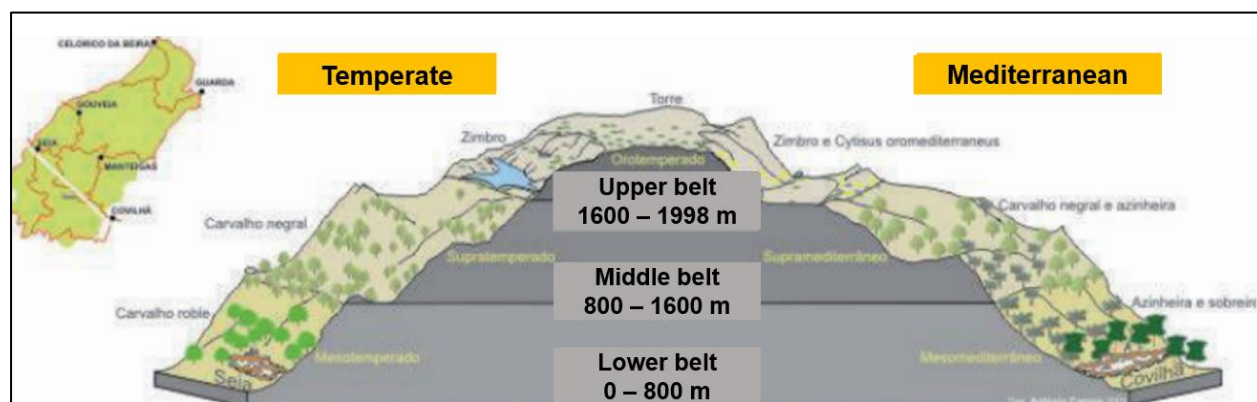


Figure 3 - Serra da Estrela divided into three altitudinal belts and Temperate/Mediterranean bio climate. Image modified from Jansen (2011).

Estrela climate occurs in the transition between Temperate and Mediterranean bioclimate (Rivas-Martínez *et al.*, 2011). It is divided into three different altitudinal belts: low (below 800m), middle (800-1600m), and upper belt (1600-1993m) (Figure 3; Vieira & Jansen, 2014). Jansen (2011) also created an additional classification based on the major types of landscape: central plateau; peaks and ridges; lower plateau; slopes and valleys, and rivers. Each one of these landscapes has different environmental conditions that allow different species to thrive. The central plateau consists mainly of dwarf shrub formations, grasslands, rocks, gravel communities, bogs, rivulets, and lakes (Jansen, 2002), with some species being strictly endemic (Jansen, 2011). The ridges and peaks usually support endemic rock fissure vegetation, with some of these areas used for wind farms (Jansen, 2011). The lower plateau is mainly covered with semi-natural biotopes like hay meadows and other grasslands, broom fields, heathlands, and fallow (rye fields). These areas are considered a well-preserved European example of an open semi-natural landscape

maintained by traditional agricultural and silvopastoral activities (Jansen, 2005); The slopes form a gradient from the higher to the lower parts of the mountain (like from one vegetation belt to another or from one biogeographic region to another (Jansen, 2002)). The highest slopes (1600-1900 meters) may carry primary grasslands and scree communities with many endemic species. There is also a sloping zone (1200-1600 meters) with degraded stages of various climax forest series, where human pressure is moderate but with no permanent settlement. On gentle or steep slopes agriculture may be practiced and numerous terraces have been constructed. Below 1200 meters the main crops found are rye, potatoes, olive groves, vineyards, orchards, and horticulture. From 1200 – 800 meters moderate to strong human pressure is observed, with scattered human settlement and afforestation. From 800 meters, population density increases, and stronger human pressure occurs (Jansen, 2011). The valleys contain riverine forests, hay meadows, aquatic and riparian vegetation, and overall water supply is provided for the human population around. Because of this, population density is higher, and crop farming is common. Some valleys may also have water reservoirs or dam constructions transformed for generating hydroelectric power, as well as supplying water for irrigation in dry periods (Jansen, 2011).

Throughout the year, the temperature in Estrela varies from -10°C to +30°C (Meteoblue, 2022). Pisani *et al.* (2019), alert that there is a “high possibility that the water resources in Serra da Estrela Mountain basin will be very vulnerable to the predicted changes in precipitation and temperature”. The mean annual and monthly temperatures will increase significantly, around 3.1 – 5.4 °C (from two different projected scenarios). This increase will be largest in the summer, and in the winter, it will reduce snow precipitation (around 54-58%) and affect the snow melting in the highest sub-basins of Estrela. Precipitation will decrease mainly in the spring, around 21-23%, and the mean annual precipitation can decrease by around 8-15%. The mean annual aquifer recharge will decrease by 12-22% and the mean annual streamflow will decrease by 10-18%. These studies are important to understand the potential impact of climate projections on the dynamics of the different habitats of Serra da Estrela.

One of the most threatened habitats of Serra da Estrela is the alpine grass habitat (“cervunais”) dominated by the species *Nardus stricta* L. The maintenance of this type of habitat is directly and indirectly associated with grazing. With a reduction of the herds, woody species like *Calluna vulgaris*, *Erica tetralix* and *Genista anglica* can potentially occupy these grassland areas. Rudley (2020) states that “warming can promote the growth of the two dominant alpine shrub species in the high plateau of Serra da Estrela Natural Park – *Juniperus communis* subsp. *alpina* and *Cytisus oromediterraneus* - but may eventually lead to changes in plant performance and distribution shifts in the longer term due to species-specific differences in the response to climatic variables.” Thus, it is increasingly important to understand which species will take advantage of global warming, potentially becoming widespread, and overtaking other species not so well adapted. One of these potential species is *Calluna vulgaris* which can occur under very different climatic conditions, indicating a high plastic potential of this species.

Calluna vulgaris in Serra da Estrela

Calluna vulgaris (L.) Hull, also known as common heather, is a small to medium-sized evergreen woody shrub, with a large geographical distribution (Figure 4a). It is native to Europe but can be found all around the world and introduced for ornamental purposes. In Portugal, it can be found in warm and dry areas, from low to high and freezing altitudes, like in Serra da Estrela (Figure 4b).

C. vulgaris dominates the so-called heathlands, which according to a report by the European Environmental Agency (EEA, 2007), are declining and vulnerable habitats. Heathlands cover about 4% of EU land, typically occurring on free-draining soil with a relatively low nutrient content and often dominated by small woody plants with herbs, mosses, liverworts, and lichens mixed (EEA, 2019). Although the heathland habitats are considered vulnerable, the dominant species, *C. vulgaris*, is not threatened and can become widespread in other types of habitats.

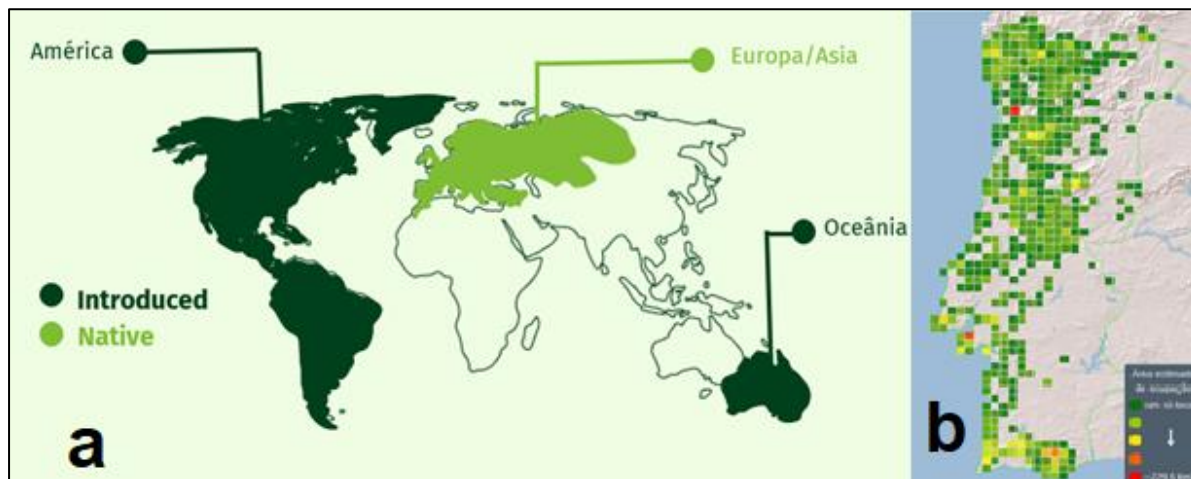


Figure 4 - a) World distribution map of *C. vulgaris*, by Invasive Species Specialist Group (ISSG) Source: issg.org/database/welcome/. b) Distribution of *C.vulgaris* in Portugal. (Source: flora-on.pt/)

Gimingham (1972) defined four ecological phases of *Calluna* structure: the pioneer phase, establishment and early development (from 0-5 years old); the building phase, where the plant is growing and dome-shaped (5-15 years old); the mature-phase, where there is a reduction in vigor but a more open canopy (15-25 years old) and the degenerate-phase, with a gap in the center with dead branches, while the outer branches are lying flat on the ground (25-30 years old). According to Lindholm (2019), *C. vulgaris* in Sweden is visited by ca. sixty insect species. In France, insect visitors belong to 58 identified species (Descamps et al., 2015). It possesses a nectarine disk under the ovary that is meant to attract pollinators like butterflies and honeybees – used in the production of dark heather honey. This species shows a high value for the ecosystem and not only provides food, but also shelter to many insects, reptiles, birds, and small mammals (Lindholm, 2019).

The first studies about altitude in *C.vulgaris*, with Grant & Hunter (1962), showed that the growth form and phenology of *C. vulgaris* changed from high to low altitudes. In high altitudes, the plants showed shorter stems, flowers had darker colors and the flowering season occurred earlier, compared with the same species at lower altitudes. This was also observed in other studies and

associated with lower temperatures at higher altitudes, leading to early flowering (Bannister, 2016). Higher altitudes are also associated with higher levels of flavonols and phenolic compounds, associated with a protective mechanism of the plant against UV radiation (Rieger *et al.*, 2008; Monschein *et al.*, 2010). Also, Hacker *et al.* (2011), hypothesized that a cushion growth form may give an advantage for frost survival in this species, with ice propagation in reproductive shoots being prevented by an ice barrier, that reduces the impact of freezing temperatures due to supercooling. When studying this characteristic in *C. vulgaris*, ice barriers were present in all reproductive stages and were extremely effective (Kuprian *et al.*, 2016). This is an important survival strategy for *C. vulgaris*, as supercooling of reproductive shoots is a mechanism that also protects developing offspring from potential frost damage. Frost can lead to cell damage and, as with low water availability, it induces cavitation affecting water flow. Also, frost can damage the cuticular surface reducing the ability of plants to control water loss (Davies *et al.*, 2010).

Wood anatomical traits of *C. vulgaris*

Woody species can “print” climatic variations in growth-rings width and other wood anatomical traits, like vessel area. Because certain woody species can live for decades or hundreds of years, depending on the species, it is possible to observe environmental trends in time and location (Guibal & Guiot, 2021). The formation of growth rings (Figure 5) is associated with the seasonal activity of the vascular cambium tissue, a secondary meristematic tissue located between the phloem and xylem, leading to the increase of perimeter in woody plants (Rathgeber *et al.*, 2016).

Wood rings are made of several types of cells with different structures and functions. Vessels have a circular section and their main function is to transport water; fibers are thick-walled cells and their main function is to give mechanical strength to the growing stem; parenchyma cells are used



Figure 5 - Transversal section of a stem of *C. vulgaris* showing one growth ring.

to store nutrients and water and function as a reserve tissue (Schweingruber, 2007) (Figure 6). The size, number, and intra-annual distribution of the cell types can vary depending on the environmental conditions (Schweingruber & Poschlod, 2005). For example, the area of the vessels can change over the year and between years. During spring and early summer, the vessel area is larger, when there is more water availability, but also when the plants have their growth peak, thus an efficient water transport system is necessary. Later in the growing season, when less water is available, there is a higher probability of cavitation (Fonti *et al.*, 2010). As water tension increases inside the xylem cells, the “trapped” air expands and fills the vessels, creating a bubble - or cavity - called an embolism. Thus, to prevent cavitation, smaller vessels are produced, increasing the proportion of fibers that are also important to mechanically sustain the growth of woody stems.

Analyzing the growth-rings width and other wood anatomical traits enables the study of the wood anatomical adjustments to the climatic conditions that can change from year to year and between sites. Thus, it is an important source of information on the plastic behavior of species that occur in different environments, like *C. vulgaris*. Correlations between the tree-ring width and temperature were already reported (Beil *et al.*, 2015) and it shows an interesting approach for analyzing abiotic conditions printed in wood.

Seasonal ring formation is identical in shrubs and trees (Schweingruber & Poschlod, 2005), but there is still much less information about the dynamics of the radial growth of shrubs, probably because they present other challenges. The growth of woody stems of shrubs is more complex: contrary to trees they do not present the main stem but several stems; growth rings are asymmetrical (can be harder to distinguish) and in some species, there is a lack of variability in ring widths from one year to the next (Ricker *et al.*, 2020), and no climatic signal can be withdrawn. Although challenging, the study of wood anatomical traits of *C. vulgaris* can give insights into the plasticity of wood, contributing to a better understanding of the strategy of some plant species to survive under contrasting conditions (like hot and freezing temperatures), as it happens with *C. vulgaris*.

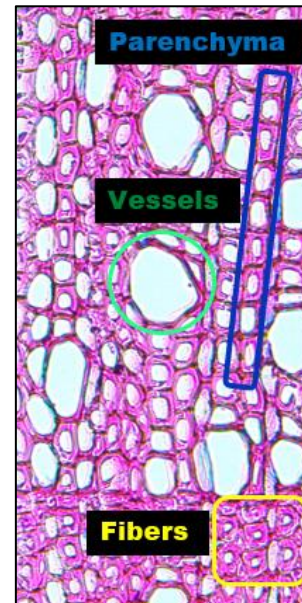


Figure 6 – Transversal section of a stem of *C. vulgaris* showing vessels (green line), fibers (yellow line) and parenchyma (blue line)

Objectives and hypothesis

This study was conducted within the project “Estrela - Effect of global warming on the diversity and functioning of the alpine ecosystems of Serra da Estrela, a threatened mountain range in the transition area between temperate and Mediterranean climates” (PTDC/BIACBI/30215/2017).

The aim was to quantify the inter-annual variability of the tree-ring width and wood anatomical traits of populations of *C. vulgaris* growing at different altitudes in Serra da Estrela. We expect that wood anatomical traits of *C. vulgaris* present high plasticity, representing a high degree of adjustment to different climatic years, and/or altitude.

Our main hypotheses are:

- Shrub-ring width decreases with altitude because the growing season is shorter;
- Vessel area decreases with altitude, due to the freezing temperatures, because larger vessels are more prone to freeze-thaw cavitation;
- The percentage of cell wall increases with altitude, increasing the mechanical strength to resist wind and snow cover.

Materials and methods

Study site and field sampling

The sampling sites (Figure 7) were defined considering the three bioclimatic belts of Estrela defined by Jansen (2011): low (below 800m); intermediate (800-1600m), and high (1600-1993m). 9 populations were chosen, 3 within each altitudinal belt, with 6 individuals randomly selected from each population. Because no populations of *C. vulgaris* were found in the lower belt of Estrela, we had to select 3 populations more distant from Estrela, nearby Coimbra. The areas chosen were: higher altitudinal belt (1868m, Covão do Boi (COV); 1862m, Sabugueiro (CUM); 1824m, Lorigã (ALX)); intermediate altitudinal belt (1680m, a caminho do Covão dos Ponchos (CAM), 1630m, Covão dos Ponchos (BUR); 1597m, Lagoa comprida (LAC)); lower altitudinal belt (345m, Carapinha da Serra (CAR); 203m, Misarela (MIS); 181m, IPARK de Coimbra (IPA)) (Figure 7).

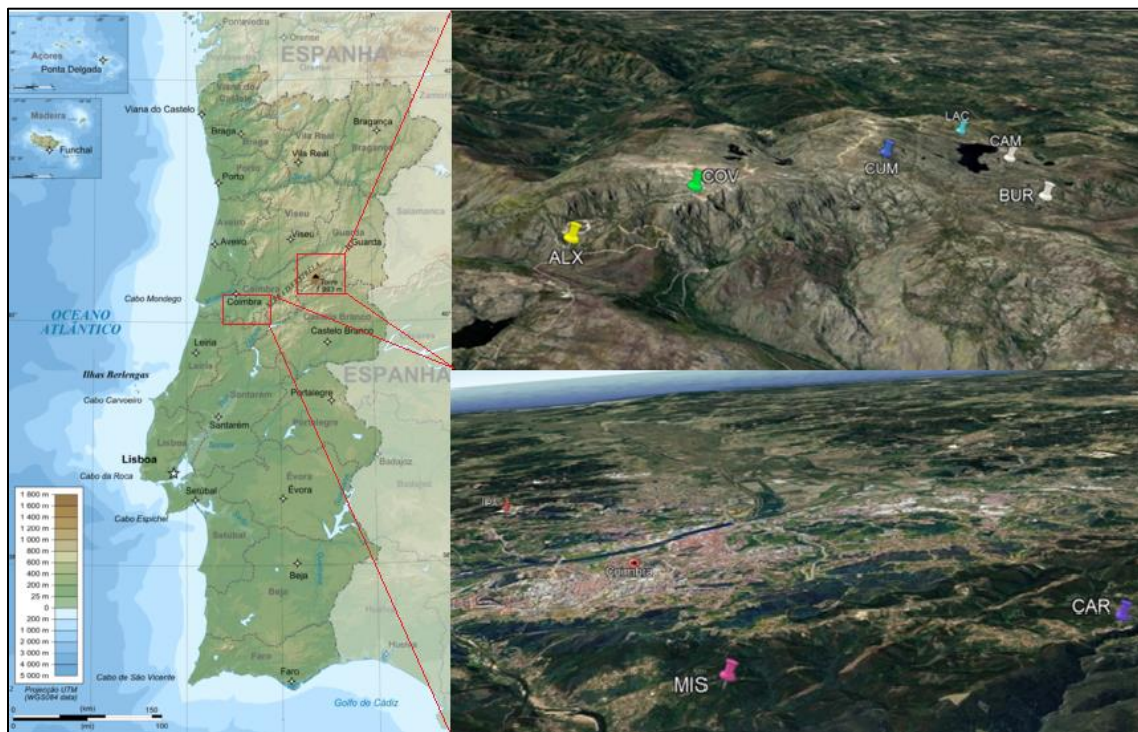


Figure 7 – Location of the sampling sites. 3D GPS made in ArcGIS program.

For each sampling site, the following additional information was recorded in a field sheet (Appendix 3): geographical coordinates, slope, and other shrub species around the selected individuals of *C. vulgaris*. In the higher and intermediate altitudinal belt, the dominant shrubs were *C. vulgaris*, *Cytisus oromediterraneus*, *C. striatus*, *Erica arborea*, and *Juniperus communis*. In the lower altitudinal belt, the dominant shrubs were *C. vulgaris*, *Erica arborea*, and *Ulex minor*. Other species were also recorded (Appendix 4). For each specimen of *C. vulgaris* the total height and diameter were measured, and three branches were cut, stored in plastic bags, and transported to the lab for further processing. A total of 162 stems were collected.

Processing of wood samples

A small piece of the stem was cut at 20 cm from the apical end of the branch (Figure 8). The same distance was kept to avoid differences in the vessel size due to allometric relations because the vessel size increases from the tip to the bottom of the branch. The samples were labeled using the following code: MIS1_R1, with the first three letters representing the sampling site (in the example MIS), the number representing the individual (1-6), R the branch (from the Portuguese “Ramo”) and the number of the branch (1-3).



Figure 8 – Wood stem sampling at 20cm of the apical end of the branch.

The wood sample was stored in histological cassettes, identified with the code of the sample, and processed through several six stages: dehydration, clearing, infiltration, embedding, cutting, and

staining. During the first stage, the wood samples were dehydrated using an increasing range of concentrations of ethanol solutions: 70% Ethanol, for 120 minutes; 90% Ethanol, for 90 minutes (2x); 95% Ethanol for 90 minutes; 100% Ethanol, 90 minutes (2x). For the second stage, the clearing agent used was Clear Rite using the following steps: 100% Ethanol with Clear Rite for 90 minutes; Clear Rite for 90 minutes (2x). All the previous steps were conducted in a fume hood. In the infiltration step, the samples were embedded in liquid paraffin in an incubator at 65°C, for 120 minutes (2x). Afterward, the samples were removed from the paraffin solution with a clamp and placed on absorbent paper to get rid of the excess paraffin solution. The paraffin embedding was made in a Shandon HistoCentre 2 station. Small metal trays were filled with hot paraffin, and with a heated clamp, the wood sample was oriented to obtain a transversal section. Afterward, the metal trays were filled with hot paraffin and immediately transferred to a freezing plate to rapidly solidify the paraffin so that the wood piece was kept in the correct position.

The paraffin blocks were cut in a rotary microtome (MICROM HM 340 E). The microtome was initially programmed to trim at 20 µm to remove the excess paraffin. Afterward, all the blocks were placed in water to hydrate for between 48 to 72 hours, depending on the wood density. The microtome was then programmed to trim at 7 µm. With the help of a small brush, the wood samples were transferred to a water bath kept at 32-34°C. The flotation bath temperature should be below the melting point of the paraffin because the aim is that the sections are readily flattened but the paraffin should not melt. Later, a microscopic slide was dived into the water at a 45° angle, while pushing the sample with the brush to the microscope slide at the same time. The microscopic slides were previously glued with glycerol gelatin. The glycerol gelatin was heated at 65°C degree in an incubator for 10 minutes. Next, a drop was placed in the center of each microscopic slide and with a glove, the drop was spread through the surface of the slide. Each slide was labeled with a pencil with the code of the sample and then placed in an incubator at 30°C overnight. The next steps were the removal of the paraffin, tissue staining, and preparation of definitive slides. Inside a fume hood, 7 glass containers were placed side-by-side with the following solutions, covering at least $\frac{3}{4}$ of the container: 4 with Clear Rite; 1 with tap water; 1 with Astra Blue and Safranin, and the last one with tap water. The samples were placed in the first two Clear Rites for

10 minutes each, and for the other two, 2 minutes each. These steps are necessary to remove the paraffin. The samples were carefully drained before changing to the next container. After this, the slides were placed in water for at least 5 minutes and then stained using Astra Blue and Safranin for 10 minutes. Then, the samples were placed in a water container to take the colorant excess (Figure 9a). For the preparation of the definitive slides, the samples were first soaked in several solutions, 5 to 10 minutes in each solution: Clear Rite; Clear Rite; Alcohol 100%, and Clear Rite again (Figure 9b). The microscopic slides were then placed in absorbent paper to remove the excess solution. 1-2 drops of Eukitt solution were placed on the top of each sample and a coverslip was pressed to remove the excessive Eukitt and any air bubbles. The microscopic slides were then stored in an incubator at 30°C overnight. All the reagents were placed for recycling afterward in a halogenated container and all the used containers were cleaned with soap and a dishwasher before being left to dry.

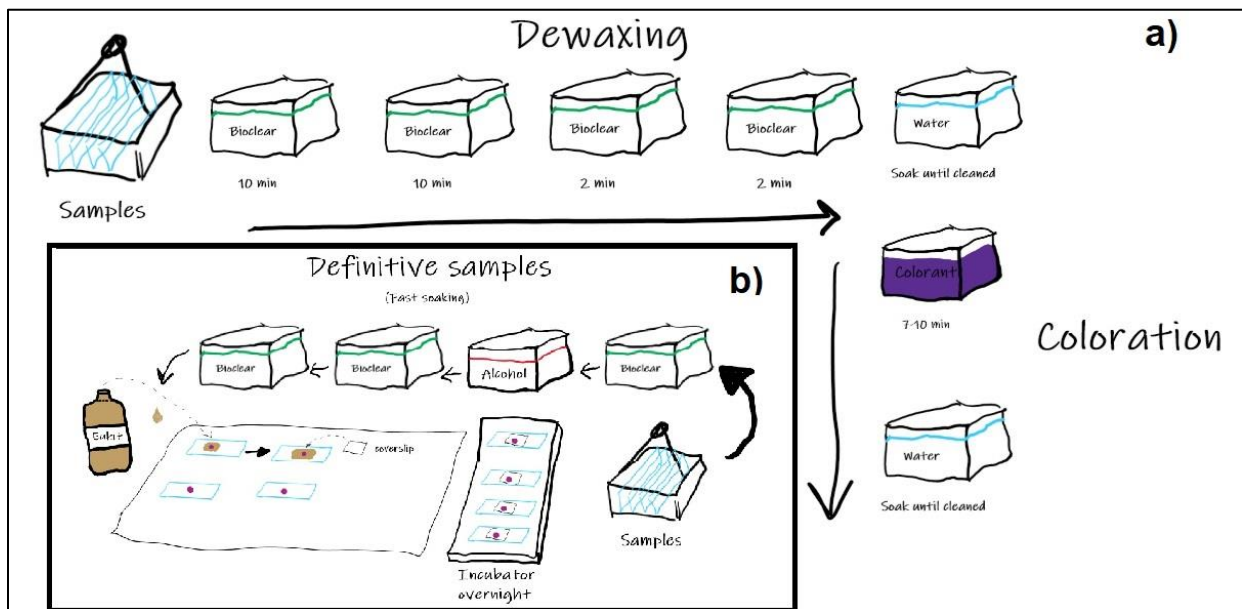


Figure 9 – Steps for (a) Dewaxing and coloration and (b) Definitive slide preparation.

Image capture and analysis

For image capture, a light microscope with a camera was used (Leica DM 4000B, with a camera Leica DFC295), attached to a computer with the Leica Application Suite, version 4.13.0. All the samples were photographed using the 5x and 20x magnifications and saved for editing. For image editing, ImageJ FIJI's plugins "Stitching" and "Weka segmentation 2D" were used. With the plugin "Stitched", multiple photographs are joined to form a unique photo. After stitching, image cuts were made for each ring section, and the image was scaled for 3.92 pixels/ μm . The function "measure" was used to measure each shrub-ring width.

The Weka segmentation allows training the program to recognize different colors and/or patterns, according to how the user teaches the program. Before image editing, photos were filtered with a "mean" filter (2.0 – 3.0 degrees), to reduce the image "noise". After filtering and using the Weka plugin, it was possible to train the program to recognize 2 types of tissue fractions: lumen vessel and cell wall (Figure 10).

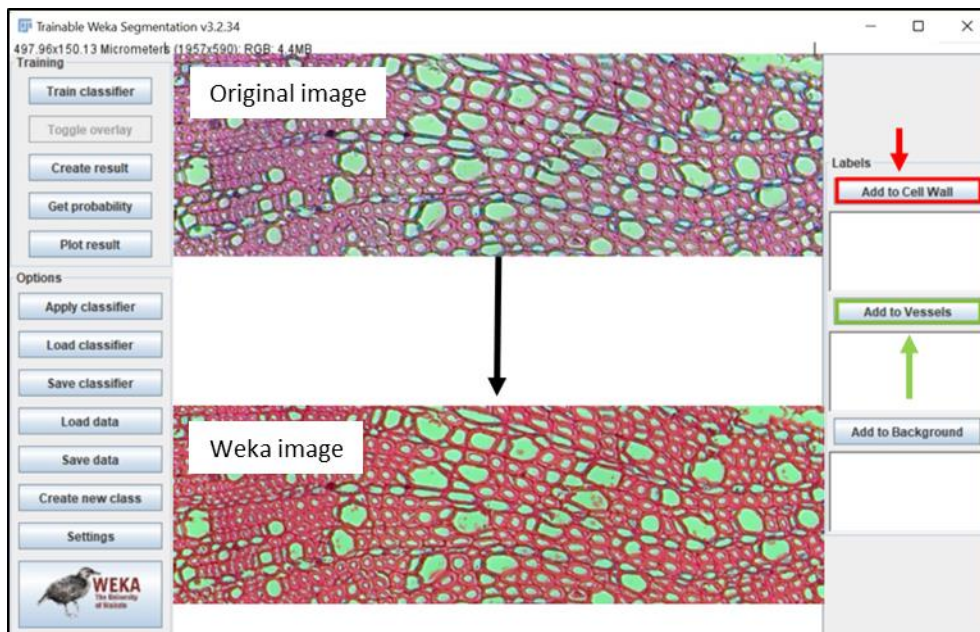


Figure 10 – Image output by Weka after training for identification of Vessels (green) and Cell walls (red).

Afterward, the WEKA image was divided into two layers, the Vessels, and Cell walls (Figure 11).

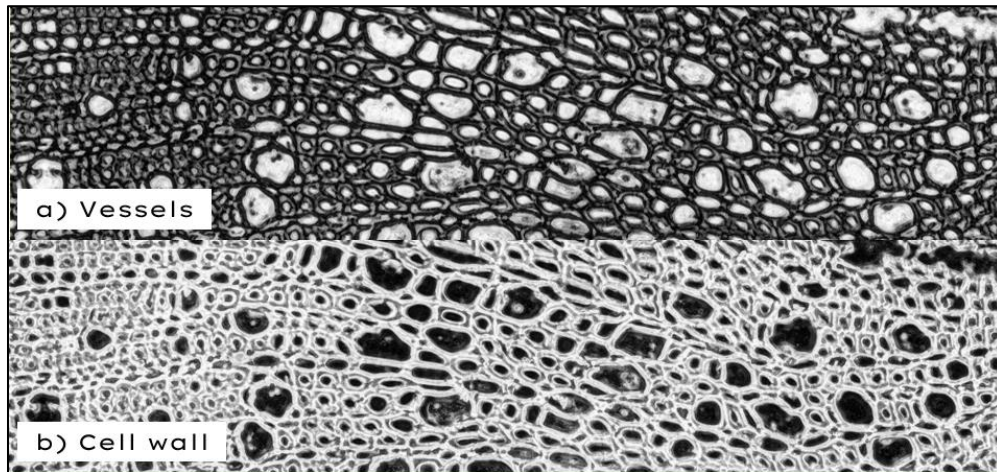


Figure 11 – Image probability output after Weka training showing two layers: a) Vessel area identified in white; b) Cell wall area identified in white.

The “Threshold” function was then used to identify the areas with vessels and cell wall, for both layers (Figure 12). In most cases, manual correction of the vessel area was necessary.

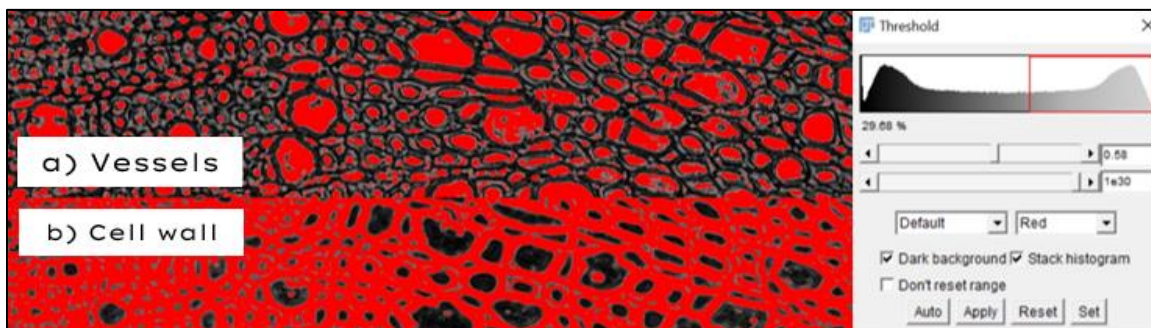


Figure 12 – The threshold function used to split the vessels from the cell wall. The “stack histogram” function was always active for a more accurate and balanced selection of areas.

The function “Analyze particles” was then used to automatically measure the individual area of all identified vessels in each growth ring (Figure 13).

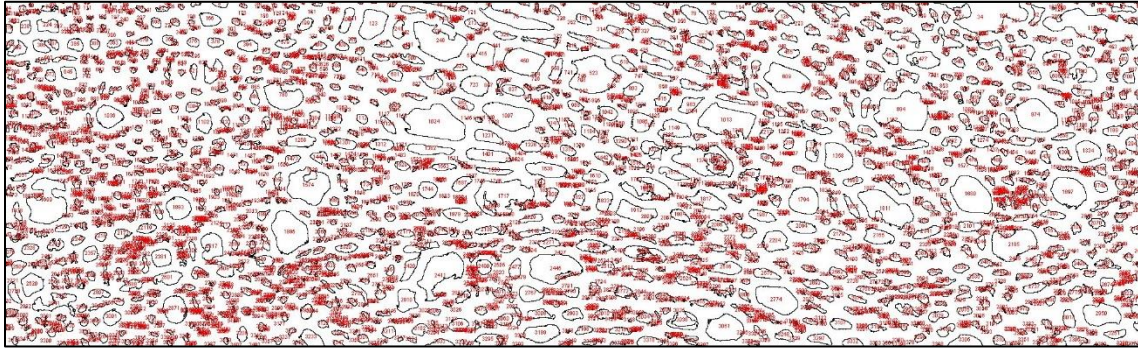


Figure 13 – Visual output of function “Analyze particles” from the vessels layer.

Statistical analysis

Climate-growth analysis

The climate data was gathered from Terra Climate 2000 R database. Monthly information regarding minimum and maximum temperature and precipitation from 2000 to 2020 was collected for climate-growth analysis (Appendix 5). According to the climate data (Appendix 5), the climatic parameters between the Mid and High sampling sites were similar. Thus, for further analysis of the climate growth relations, the populations from the Mid and High sampling sites were analyzed together.

The growth series of each specimen of the populations from Low and Mid + High sampling areas were cross-dated using a visual and statistical assessment. For the statistical assessment, the Pearson correlation was used to identify the highest correlations between the growth series (Appendix 6 and Appendix 7). This analysis was first performed by site and then among the sites for each altitude (Low and Mid + High). After the visual and statistical analysis, some individuals were removed because their growth patterns were very different, selecting the specimens with the

best agreement in the growth series. Then an average growth curve was obtained for the Low and Mid + High sampling areas for further analysis with the climatic parameters.

The R package DendroTools has linear and nonlinear methods for analyzing monthly dendroclimatological data, which was used for correlating climate-growth analysis. The correlation test used by the package was the “Pearson’s correlation test”, which tests if and which climatic variables can affect the SRW.

Wood traits and altitude

As the number of shrub rings was different between the sampling areas, only the last 5 common years were used in the statistical analysis to test the effect of the altitude in the shrub ring width (SRW), average vessel area (AVA), and percentage of the cell wall (PCW). Because the growth ring from 2021 was incomplete in some of the sampling areas, the analyzed period was from 2016 to 2020. The three variables used (SRW, AVA, and PCW) were tested for normality with the Shapiro-Wilk test in R. After testing, only PCW showed normally distributed data, with a p-value higher than 0.05 (p-value = 0.2352). SRW and AVA p-values were below 0.05 (2.18e-13 and 0.02627, respectively), which means they did not follow a normal distribution and therefore a transformation of the data was needed. The best results were with log transformation for SRW variable (p-value = 0.3547) and square transformation for AVA variable (p-value = 0.1915).

Because stem age can affect the SRW, with younger stems showing wider SRW, compared with older stems, regression analysis between age and log SRW was performed, and the residuals were used for further analysis. With this procedure, the effect of age on SRW was removed.

Linear mixed models (LMM) were used for each of the dependent variables (residuals of SRW, AVA square, and PCW transformed) using altitude as a fixed factor, and year and local as a random factor. All models showed little residuals, meaning that the models represent a good fit for our data. After confirming the fitness of the models, variance analysis was made with a two-way ANOVA test.

Results

Age, height, and diameter of *C. vulgaris*

Table 1 presents the height and diameter of *C. vulgaris* for each local and altitude. On average, individuals were shorter and wider at the highest altitudes, and taller and narrower at the lowest altitudes.

Table 1 – Height and diameter of *Calluna vulgaris* for each local and altitude. Mean \pm SE. For more information regarding individuals, check Appendix 8 and Appendix 9.

<i>Elevation</i>	<i>Local</i>	<i>Altitude (m)</i>	<i>Age (years)</i>	<i>Height (cm)</i>	<i>Diameter (cm)</i>
High	COV – Covão do boí	1868	9.72 \pm 0.59	25.17 \pm 1.67	161.00 \pm 16.12
	CUM – Sabugueiro	1862	9.44 \pm 1.26	23.00 \pm 2.68	99.67 \pm 6.33
	ALX – Lorigã	1824	13.50 \pm 1.03	34.33 \pm 2.80	122.17 \pm 9.63
	Mean	1851 \pm 14	10.89 \pm 0.63	27.50 \pm 1.82	127.61 \pm 8.90
Mid	CAM – On the way to BUR	1680	10.89 \pm 0.79	52.33 \pm 5.18	96.83 \pm 3.62
	BUR – Covão dos conchos	1630	13.00 \pm 0.80	42.83 \pm 5.18	127.83 \pm 5.18
	LAC – Lagoa comprida	1598	13.41 \pm 1.16	29.17 \pm 2.18	106.67 \pm 3.85
	Mean	1636 \pm 24	12.40 \pm 0.56	41.44 \pm 3.10	110.44 \pm 4.38
Low	CAR – Carapineira da Serra	345	6.24 \pm 0.46	119.00 \pm 10.45	111.50 \pm 10.04
	MIS – Misarela	203	6.56 \pm 0.59	85.17 \pm 9.48	50.50 \pm 6.55
	IPA – IPark Coimbra	181	4.75 \pm 0.30	58.33 \pm 1.76	48.50 \pm 3.05
	Mean	243 \pm 51	5.86 \pm 0.29	87.50 \pm 7.53	70.17 \pm 8.03

Climate-growth analysis

As mentioned in materials and methods, the available climatic data showed no significant differences between the Mid and High sampling sites. Thus, for the climate-growth analysis of Mid and High sampling sites, the same climatic data was used.

For the last 20 years, the average annual maximum temperature for the Low, and Mid + High sites was 20.8°C, and 12.1°C respectively (Figure 14). The hottest month in Low, and Mid + High was August, with 28.7°C and 21.7°C. The average annual minimum temperature for the Low and Mid + High and Low sites was 10.7 °C, and 4.8 °C respectively. The coldest month for the Low sites was January with 5.6°C, and the Mid + High was February, with -1.4 °C. The total annual precipitation for the Low sites was 1062mm, and for the Mid + High sites was 1763mm. The months with the higher and lower precipitation in the Low and Mid + High sites were October and July, respectively.

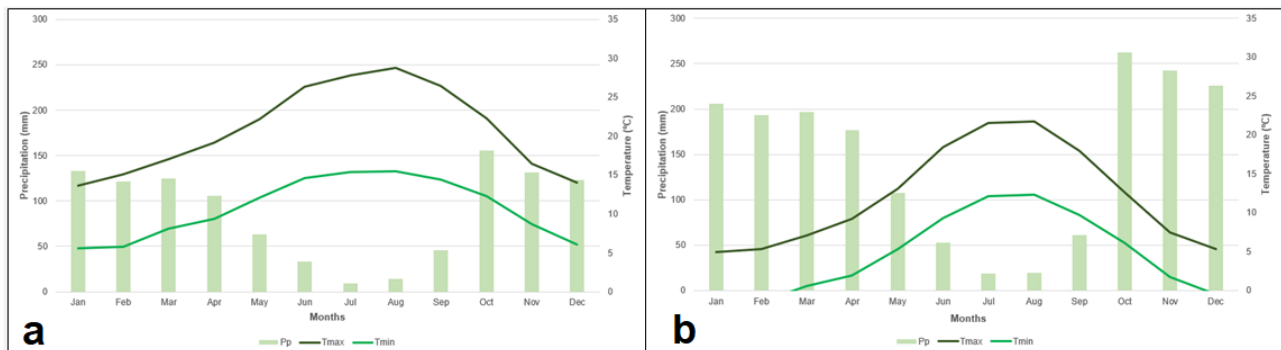


Figure 14 – Climatic diagram of annual mean maximum temperature (T_{max}), minimum temperature (T_{min}), and precipitation (P_p) in (a) Low and (b) Mid + High sampling sites for the period 2000 - 2020. Source: TerraClimate dataset

Figure 15 shows the average annual maximum and minimum temperature, and the total annual precipitation of the last 20 years in the Low and Mid + High sites. In the last 20 years, the year with the highest maximum temperature in Low and Mid + High sites was 2017, with 22.1 °C and

13.3 °C, respectively. The lowest minimum temperature in Low and Mid + High sites was recorded in 2015, with 10.1 °C and 4.3 °C, respectively. The year with the highest and lowest precipitation in the Low sites was 2010 and 2005, respectively. For the Mid + High sites the highest precipitation was recorded in 2010 and the lowest in 2005.

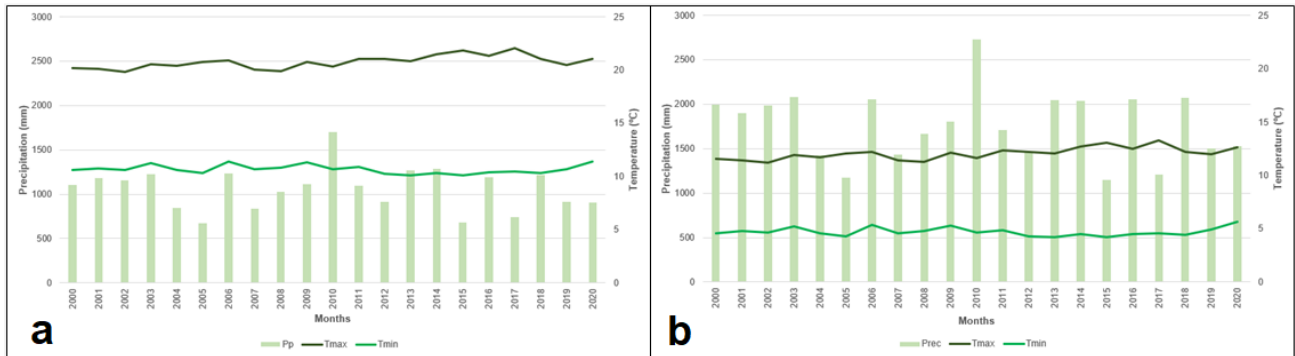


Figure 15– Climatic diagram of annual mean maximum temperature (T_{max}), minimum temperature (T_{min}), and total annual precipitation (P_p) in (A) Low and (B) Mid + High sites, for the period 2000 - 2020. Source: TerraClimate dataset

The climate-growth analysis was made using the average growth curves for the Low and Mid + High sites (Figure 16). The average growth curve for Low sites ranging from 2015 to 2020 (5 years), and for the Mid + High sites ranged from 2004 to 2020 (16 years).

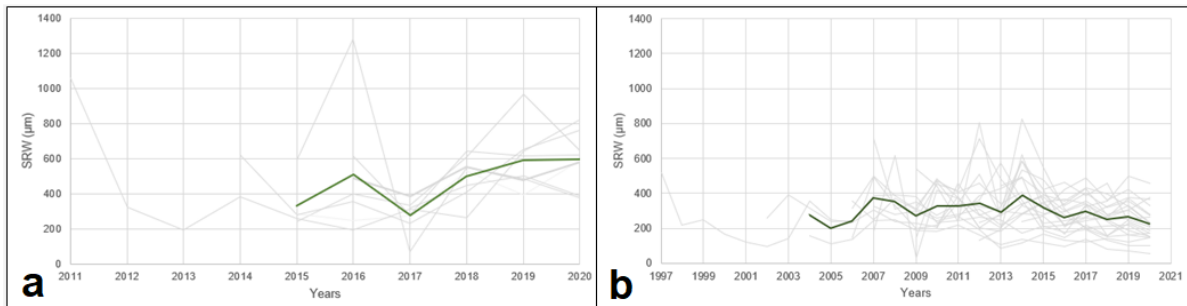


Figure 16 – Growth curves of individuals (grey lines) and average growth curve (green line) in (a) Low and (b) Mid + High sites.

The year with the highest and lowest SRW in the Low sites was 2020 and 2017, respectively. For the Mid + High sites the year with the highest SRW was 2014, and the lowest SRW was recorded in 2005.

Table 2 shows the most significant climate-growth correlations between climatic parameters and SRW. For Mid + High sites, SRW showed a negative marginal significant correlation with the maximum temperature of July, a negative significant correlation with the minimum temperature from July to August, and a positive correlation with the precipitation from May to September. For the Low sites, only marginal significant correlations were found, a negative one with the maximum temperature from June to August, and a positive significant correlation with the minimum temperature in January.

Table 2 - Table with results from Pearson correlation coefficients between SRW and climatic variables (mean monthly values) in Mid + High and Low sites. * $p < 0.1$, ** $p < 0.05$.

	Mid + High (2004-2020)	Low (2011-2020)
Tmax	July (-0.43) *	Jun-Aug (-0.802) *
Tmin	July-Aug (-0.716)**	Jan (0.582) *
Precipitation	May-Sept (0.701)**	-

The effect of altitude on wood anatomical traits

To understand if the altitude influenced the wood anatomical traits of *C. vulgaris*, and since individuals from the different sites showed different ages, we have restricted the comparison from 2016 to 2020. Table 3 presents the average values for the SRW, AVA, and PCW by local and altitude for the period 2016 to 2020, as well as the average age of the branches.

Table 3 - Shrub-ring-width (SRW), average vessel area (AVA), and cell wall percentage (PCW) of *C. vulgaris* from different locals and altitudes for the period 2016-2020. Age refers to the average age of the branches. Mean \pm SE. For more information regarding individuals, check Appendix 9.

<i>Elev</i>	<i>Local</i>	<i>Altitude(m)</i>	<i>Age (years)</i>	<i>SRW (μm)</i>	<i>AVA (μm²)</i>	<i>PCW (%)</i>
High	COV	1868	9.72 \pm 0.59	274.58 \pm 14.14	43.57 \pm 1.40	59.60 \pm 0.89
	CUM	1862	9.44 \pm 1.26	269.26 \pm 15.72	34.13 \pm 1.26	72.39 \pm 0.50
	ALX	1824	13.50 \pm 1.03	275.07 \pm 14.32	43.92 \pm 1.30	61.46 \pm 0.67
	Mean	1851 \pm 14	10.89 \pm 0.63	273.00 \pm 32.83	40.71 \pm 3.13	64.27 \pm 2.06
Mid	CAM	1680	10.89 \pm 0.79	320.16 \pm 12.39	38.45 \pm 0.77	65.33 \pm 0.52
	BUR	1630	13.00 \pm 0.80	202.18 \pm 11.25	36.46 \pm 1.02	60.77 \pm 0.79
	LAC	1598	13.41 \pm 1.16	241.97 \pm 12.24	39.73 \pm 1.13	66.22 \pm 0.75
	Mean	1636 \pm 24	12.40 \pm 0.56	256.03 \pm 28.78	38.22 \pm 2.16	64.13 \pm 1.61
Low	CAR	345	6.24 \pm 0.46	488.32 \pm 34.47	40.33 \pm 1.41	66.63 \pm 1.19
	MIS	203	6.56 \pm 0.59	345.56 \pm 31.97	31.01 \pm 0.96	68.59 \pm 0.86
	IPA	181	4.75 \pm 0.30	456.72 \pm 32.42	45.92 \pm 2.30	71.47 \pm 0.76
	Mean	243 \pm 51	5.86 \pm 0.29	431.01 \pm 69.69	38.99 \pm 3.63	68.80 \pm 2.06

Figure 17 shows the SRW from 2016 to 2020, comparing the Low, Mid, and High sites. Although the Low site presented higher SRW, compared to the Mid and High sites, when the age effect was removed from the SRW, no statistical differences were observed (Table 4).

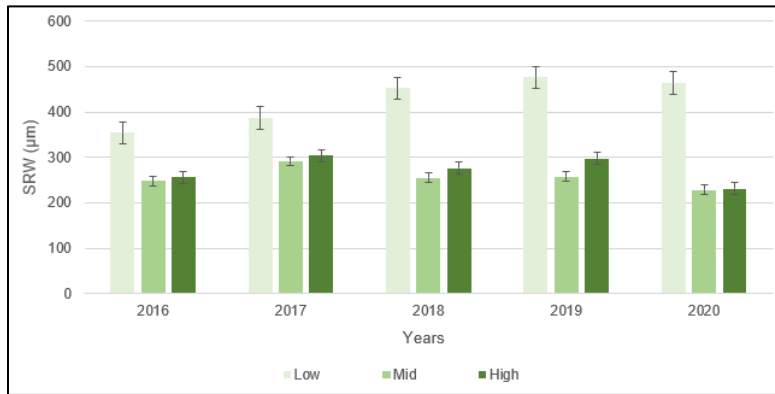


Figure 17 – Shrub-ring width (SRW) from 2016 to 2020 at Low, Mid, and High sites. Error bars represent the SE.

Table 4 - Summary of the linear mixed-effects models of the influence of altitude, local, and year on the variation of the wood trait parameters (SRW, AVA, and PCW). For more information regarding the AVA and PCW, consult Appendix 11 and Appendix 12.

<i>SRW Model format for R program: lmer(Residuals ~ Elev + (1 Ano) + (1 Local))</i>					
<i>AVA and PCW Model format for R program: lmer(Variable ~ Elev + (1 Ano) + (1 Local))</i>					
Model	N par	Sum sq	Mean sq	F value	P value (0.05)
SRW_model		<i>For more information, consult Appendix 10</i>			0.256
AVA_model	2	0.160	0.080	0.201	0.993
PCW_model	2	48.375	24.188	1.121	0.347

Figure 18 shows the AVA from 2016 to 2020, comparing the Low, Mid, and High sites. No significant differences were found between the Low, Mid, and High sites, and years.

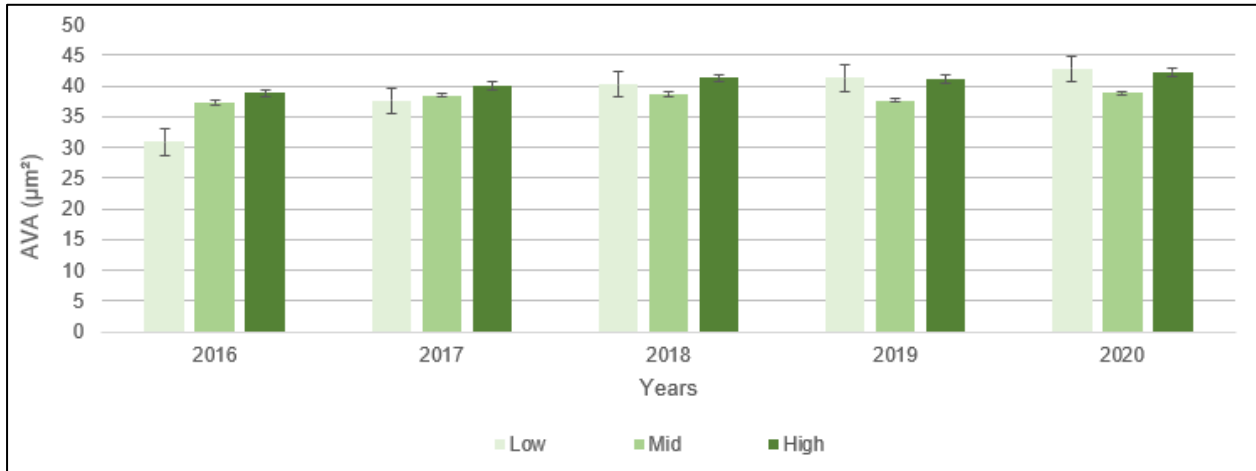


Figure 18 - Average vessel area (AVA) from 2016 to 2020 at Low, Mid, and High sites. Error bars represent the SE.

Figure 19 shows the percentage of the cell wall (PCW) between the three elevations, for the 2016-2020 period. The PCW didn't show significant differences along sites or years.

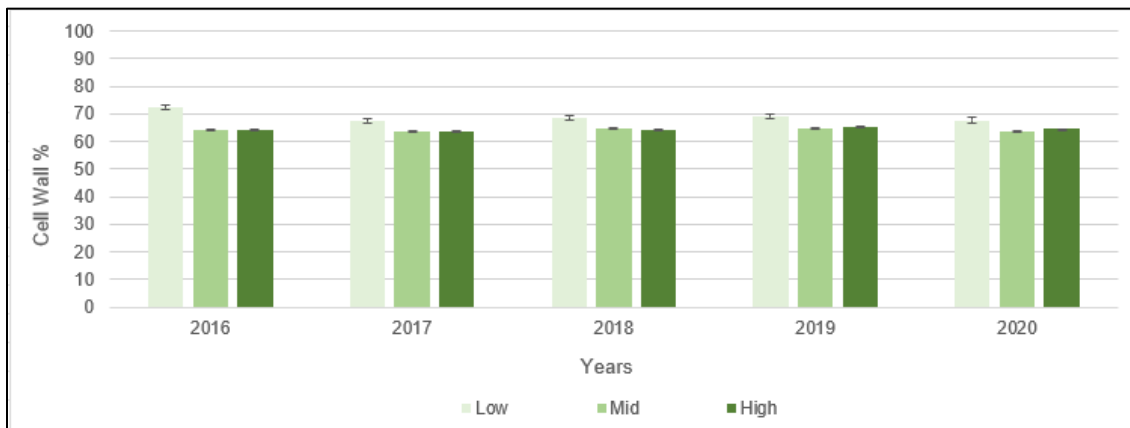


Figure 19 - Percentage of the cell wall (PCW) from 2016 to 2020 at Low, Mid, and High sites. Error bars represent the SE.

Vessel area distribution frequency

Although the AVA was not significantly different between the Low, Mid, and High sites (Figure 18), there was a slight tendency for the High sites to have a higher AVA. To check if High sites present larger vessels, a frequency distribution of the vessel area was made, considering only the lumen areas higher than $90\mu\text{m}^2$ (Figure 20). The decision to only use lumen areas higher than $90\mu\text{m}^2$ was related to their higher hydraulic capacity. The Low sites showed 41.8% of their vessels within the size class between 90 and $168\mu\text{m}^2$, while Mid and High sites showed 29.9% and 32.7%, respectively. The % of vessels $>790\mu\text{m}^2$ was 1.9%, 1.8%, and 3.4% in the Low, Mid, and High sites, respectively.

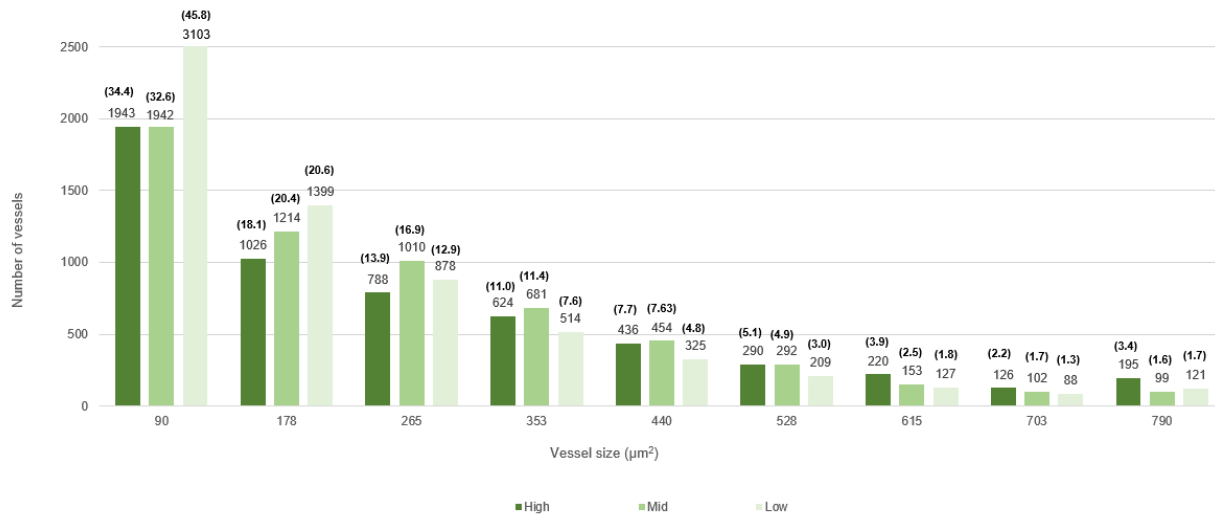


Figure 20 - Vessel area frequency distribution in the Low, Mid, and High sites. In brackets the value in percentage.

Discussion

Age, height, and diameter of *C. vulgaris*

The branches collected from the populations at the Mid and High sites were in general older, compared with the Low sites. Probably at Low sites, the disturbance is higher and consequently, the populations are younger. The height and diameter of *C. vulgaris* shrubs decreased and increased, respectively, with altitude. Altitudinal gradients have a significant impact on plant height for all herbaceous plants, shrubs, and trees, decreasing significantly as altitude increases (Mao *et al.*, 2018). With increasing altitude, shrubs are subjected to stronger winds, and snow cover. Thus, the habit of a smaller height and larger diameter probably diminishes the risk of mechanical damage. The Low sites were occupied by trees, thus a higher height of *C. vulgaris* can be advantageous to receive more light. In another study made in Serra da Estrela, Lacerda (2020) showed that the volume of *Juniperus communis* decreased with altitude, while for *Cytisus oromediterraneus* the volume increased. The volume depends on the height and diameter, as shown in the formula to calculate the volume of a cylinder: $V = \pi d^2h/4$, where d is the diameter and h is the height. Thus, the volume can increase if height and/or diameter increase. The growth of shrubs is also dependent on plant competition for space. The increasing volume of *C. oromediterraneus* with altitude can simply be related to decreasing competition with altitude and it can spread more in diameter, for example. In the case of *C. vulgaris*, when calculating the average volume of the populations from Low, Mid, and High sites, and assuming the cylindrical shape, it gives a volume of 0.422m^3 , 0.149m^3 , and 0.076m^3 , respectively. Thus, in the case of *C. vulgaris*, the volume also decreases with altitude. Although generally there is a decreasing trend of plant height with altitude, Moles *et al.* (2009), suggest that globally, latitude can be a better predictor of plant height than altitude. There are thresholds, or breakpoints, that dictate patterns of plant height implying that there are more unknown environmental factors to consider when studying the relation of plant height with altitude.

Growth series and climate correlations

The growth series length for the Mid + High sites was 16 years (from 2004-2020), while for the Low sites was only 5 years (2015 - 2020). The short time length of the Low sites limited the correlations with climatic conditions, with the correlations found to be marginally significant ($p < 0.1$). Anyway, *C. vulgaris* from all altitudes (High, Mid, Low) showed a negative correlation with the summer temperature. Low sites also showed a marginal positive correlation with the minimum temperature in January. Mid + High sites showed a positive correlation with precipitation from May to September. Notably, summer drought under the Mediterranean climate limits wood growth with high temperatures in summer increasing evapotranspiration. Thus, plants need to control the water loss, closing their stomata and consequently reducing the carbon uptake, that is needed to build the woody stems. Several studies on shrubs present a positive correlation for growth in warm summers at high elevations or altitudes (Hallinger *et al.*, 2010; Blok *et al.*, 2011; Weijers *et al.*, 2012). Another study made in the Faroe Islands showed that the growth of *C. vulgaris* was strongly positively correlated with winter and summer temperatures (Beil *et al.*, 2015). The climate in the Faroe Islands is hyper-oceanic, with high annual precipitation, cool summers, mild winters, and small differences between the seasons (Beil *et al.*, 2015). Thus growth-climate sensitivity is then quite different when compared with *C. vulgaris* growing under a Mediterranean climate. This reinforces the role of climate on wood growth dynamics, with *C. vulgaris* adjusting to the prevailing climatic conditions. This can indicate that different populations of *C. vulgaris* can develop adaptive traits to local climates as mentioned in Meyer-Grünefeldt *et al.* (2016).

Calluna vulgaris from Low sites showed a positive marginal correlation with the minimum temperature of January. This can indicate that if the temperatures in the winter are higher, growth can start earlier, and wider growth rings can be formed because of a larger time window to grow. This correlation would be unlikely to occur at the Mid and High sites because minimum temperatures in January are below zero, due to the altitude effect, and thus it is not possible to reactivate the cambial activity.

A precipitation signal was found in the populations of Mid + High sites, with a positive correlation with precipitation from May to September. This indicates that water availability in spring and summer is central to the wood growth of *C. vulgaris*. Cabon *et al.* (2020) studied the wood growth dynamics of *Larix decidua* and *Picea abies* along an altitudinal gradient between 1300 and 2200m a.s.l, in the central Swiss Alps, and showed that temperature was the trigger for the onset of tracheid production, and water availability determined the end and total amount of tracheids produced annually. Rahman *et al.* (2020) showed that the reactivation of cambial activity in the conifer *Chamaecyparis pisifera*, from temperate climates, is achieved when the accumulated temperature is above a threshold of 13°C. This indicates that the annual pattern of temperature accumulation from late winter to early spring is central to determining cambial reactivation (Rahman *et al.*, 2020).

A warmer climate it's expected for the next years globally (Jia *et al.*, 2018), which will influence the phenology of shrubs (Lacerda, 2020), but also herbs (Dee & Stambaugh, 2019), and trees (Begum *et al.*, 2018). Because the radial growth of dwarf shrubs is influenced by climatic regional conditions (Gazol & Camarero, 2012), the impact of increasing temperatures can induce an earlier reactivation of the cambial activity, especially in higher altitudes where winter temperature is an important limiting factor. Increasing temperature can also increase evapotranspiration in spring and summer, potentially increasing water stress, and this is especially important in mountain areas under the Mediterranean climate. Ibe *et al.* (2020) showed that the response of *C. vulgaris* to an increase in vapor pressure deficit (VPD) strongly depended on the provenance of the population. Wang *et al.* (2020), in a long-term study about changes in growth patterns in alpine grassland plant communities, showed that climate change promoted shorter and faster growth periods, with earlier phenology, but without changes in the annual biomass production. Peguero-Pina *et al.* (2020) also state that the response of plant species to climate change also depends on the level of morphological and physiological plasticity. In the case of *C.vulgaris*, when studied in response to extreme weather events like drought and heavy rain (Walter *et al.*, 2016), it showed a strong negative impact on seed germination rate and timing, which can affect future seedlings and the survival of a plastic species like *C.vulgaris*.

Impact of altitude on SRW, AVA, and PCW

C. vulgaris growing at different altitudes showed no significant differences in SRW, AVA, and PCW. Independently of the different climatic conditions, age, type and depth of soil, and other possible local environmental differences, the morphological traits of wood were similar.

We would expect that *C. vulgaris* growing at higher altitudes would show a lower SRW because the length of the growing season is shorter due to the limiting temperatures at higher altitudes (Körner, 2003). Although the raw values of SRW showed that the growth width was wider in the Low site, compared with the Mid and High sites, we cannot conclude that this was caused by an altitude effect because the populations at the Low sites were much younger. Younger stems show wider rings and as they grow older the ring width diminishes, a known allometric relation known in dendrochronological science (Weiner, 2004). Thus, when the effect of age was removed from SRW, using the residuals of the regression between SRW and age, no differences were observed in the SRW between the different altitudes. The final width of a growth ring might depend on the length of the growing season but also the rate of cambial division and xylem development (Ren *et al.*, 2019). Dietz *et al.* (2004) findings reinforce the idea that the length of the vegetation season is not related to growth, at least in the long run, for perennial plants. Thus, *C. vulgaris* growing at higher altitudes, with a shorter growing season, might present a higher growth rate and no differences in the SRW occur when compared with the populations growing at lower altitudes.

We would also expect that the AVA would be smaller at higher altitudes, but no differences occurred between the Low, Mid, and High sites. At high altitudes, trees tend to show narrow vessels, while at low altitudes, trees present wider vessels (Yang, 2020). Larger vessels are more prone to cavitation if subjected to freeze-thaw cycles during the winter season, as occurs at high altitudes (Pitterman & Sperry, 2006). Ice formation in the sap leads to the creation of air bubbles in the vessels and when the sap melts, the bubbles can nucleate leading to a gas-filled (embolized) conduit that prevents water transport (Pitterman & Sperry, 2006). However, *C. vulgaris* does not present smaller vessels at higher altitudes, and populations from the High sites even showed a higher percentage of the bigger vessels ($>790 \mu\text{m}^2$). Larger vessels at the beginning of the growing

season can lead to higher growth rates, because of a higher capacity to transport water and thus able to keep the stomata open for CO₂ uptake. This could be a useful strategy for sites where the growing season length is shorter, even at the cost of those large vessels becoming embolized in the following winter. However, it was not observed many tyloses, a visual sign of embolism, although it was not quantified the number of tyloses per area. Snow cover can also insulate the shrubs from freezing temperatures, avoiding sap freezing. *C. vulgaris* also presents anti-freeze strategies presenting an ice barrier that allows water conductivity while blocking the ice from entering the plant (Jacobsen *et al.*, 2019) and large volume vessels only embolizing at a higher water potential (Kuprian *et al.*, 2016). Interestingly, the populations from Low sites showed a higher percentage of smaller vessels, between 90-168 μm^2 , compared with Mid and High sites. At lower altitudes the growing season is longer, and, under the Mediterranean climate, the summer water stress can induce cavitation, with smaller vessels being more resistant to water stress cavitation (Jacobsen *et al.*, 2019). A study on the vulnerability to cavitation during the summer of six species of subalpine dwarf shrubs showed that *C. vulgaris* was one of the most vulnerable to cavitation (Ganthaler & Mayr, 2021).

The PCW was similar between the Low, Mid, and High sites. This parameter can be used as an indirect measure of mechanical strength and the occurrence of cell fibers that, in angiosperms, have very thick walls. Some studies showed that wood dry density and cell wall thickness increased with altitude (Kiaei *et al.*, 2019) but other studies showed the opposite results (Gülsoy, 2021). At higher altitudes, the strong winds and snow cover represent mechanical stress for alpine shrubs, thus we would expect a higher percentage of the cell wall at higher altitudes. However, the growth habit at higher altitudes, with a lower height and larger diameter, can reduce the impact of winds. A cushion shape also prevents the break-off branches from the snow weight. In a study with *Picea abies*, Piermattei *et al.* (2020) showed that mechanical wood anatomical traits are mainly influenced by age, with older trees showing thicker cell walls. Nonetheless, trees from different altitudinal ranges, with different mean temperatures and total precipitation, showed small changes in the wood anatomical traits (Piermattei *et al.*, 2020).

Conclusions

Climate-growth correlations were slightly different between the Low and Mid + High sites. A common signal was the negative correlation with summer temperature, which is expected under a Mediterranean climate. The Low site populations showed a marginal positive correlation with the minimum temperature in January, indicating the possibility of an earlier start of the growing season. The Mid + High populations showed a positive correlation with precipitation from May to September indicating that water availability in spring and summer is important for wood growth.

The wood anatomical traits SRW, AVA, and PCW measured in the last five years, from 2016-2020, showed no significant differences between the Low, Mid, and High populations of *C. vulgaris*. This indicates that the measured wood anatomical traits are highly conserved, even when shrubs are subjected to different environmental conditions. Nonetheless, it seems that populations from High sites tend to have a higher percentage of wider vessels.

The increasing temperature predicted by climate change projections will probably have impacts on the growth dynamics of *C. vulgaris*. Populations at higher altitudes will probably start the growing season earlier, as they are limited by lower temperatures, but water stress in summer will increase, precluding wood growth in both low and high-altitude populations of heather. If wider vessels are an adaptive trait of high-altitude populations to a shorter growing season, under a scenario of water stress increase, wider vessels can increase the susceptibility to cavitation.

Shrubs are complex structures in terms of growth, compared with trees, and with fewer studies on wood anatomical traits and dendrochronology. However, shrubs are a very important and dominant functional group in alpine and Mediterranean areas. Thus more studies are necessary to understand their growth dynamics and adaptive traits, especially under scenarios of climate change.

References

- Alam, M. K. (2021). Climate change, biosystematics and taxonomy. *Bangladesh Journal of Plant Taxonomy*, 28(1), 277–287. <https://doi.org/10.3329/bjpt.v28i1.54223>
- Alexander, J. M., Chalmandrier, L., Lenoir, J., Burgess, T. I., Essl, F., Haider, S., Kueffer, C., McDougall, K., Milbau, A., Nuñez, M. A., Pauchard, A., Rabitsch, W., Rew, L. J., Sanders, N. J., & Pellissier, L. (2018). Lags in the response of mountain plant communities to climate change. In *Global Change Biology* (Vol. 24, Issue 2, pp. 563–579). Blackwell Publishing Ltd. <https://doi.org/10.1111/gcb.13976>
- Bannister, P. (2016). *Flowering and Shoot Extension in Heath Plants of Different Geographical Origin*. 66(1), 117–131.
- Begum, S., Kudo, K., Rahman, M. H., Nakaba, S., Yamagishi, Y., Nabeshima, E., Nugroho, W. D., Oribe, Y., Kitin, P., Jin, H. O., & Funada, R. (2018). Climate change and the regulation of wood formation in trees by temperature. In *Trees - Structure and Function* (Vol. 32, Issue 1, pp. 3–15). Springer Verlag. <https://doi.org/10.1007/s00468-017-1587-6>
- Beil, I., Buras, A., Hallinger, M., Smiljanić, M., & Wilmking, M. (2015). Shrubs tracing sea surface temperature—*Calluna vulgaris* on the Faroe Islands. *International Journal of Biometeorology*, 59(11), 1567–1575. <https://doi.org/10.1007/s00484-015-0963-4>
- Blok, D., Sass-Klaassen, U., Schaepman-Strub, G., Heijmans, M. M. P. D., Sauren, P., & Berendse, F. (2011). What are the main climate drivers for shrub growth in Northeastern Siberian tundra? *Biogeosciences*, 8(5), 1169–1179. <https://doi.org/10.5194/bg-8-1169-2011>
- Cabon, A., Peters, R. L., Fonti, P., Martínez-Vilalta, J., & de Cáceres, M. (2020). Temperature and water potential co-limit stem cambial activity along a steep elevational gradient. *New Phytologist*, 226(5), 1325–1340. <https://doi.org/10.1111/nph.16456>

Coelho, S., Rafael, S., Lopes, D., Miranda, A. I., & Ferreira, J. (2021). How changing climate may influence air pollution control strategies for 2030? *Science of the Total Environment*, 758. <https://doi.org/10.1016/j.scitotenv.2020.143911>

Dahl, M. B., Peršoh, D., Jentsch, A., & Kreyling, J. (2021). *Root-Associated Mycobiomes of Common Temperate Plants (Calluna vulgaris and Holcus lanatus) Are Strongly Affected by Winter Climate Conditions*. <https://doi.org/10.1007/s00248-020-01667-7/Published>

Davies, G. M., Legg, C. J., O'Hara, R., MacDonald, A. J., & Smith, A. A. (2010). Winter desiccation and rapid changes in the live fuel moisture content of *Calluna vulgaris*. *Plant Ecology and Diversity*, 3(3), 289–299. <https://doi.org/10.1080/17550874.2010.544335>

Dee, J. R., & Stambaugh, M. C. (2019). A new approach towards climate monitoring in Rocky Mountain alpine plant communities: A case study using herb-chronology and *Penstemon whippleanus*. *Arctic, Antarctic, and Alpine Research*, 51(1), 84–95. <https://doi.org/10.1080/15230430.2019.1585173>

Descamps, C., Moquet, L., Migon, M., Jacquemart, A. L., & Brunet, J. (2015). Diversity of the insect visitors on *Calluna vulgaris* (Ericaceae) in southern France heathlands. *Journal of Insect Science*, 15(1). <https://doi.org/10.1093/jisesa/iev116>

Dietz, H., von Arx, G., & Dietz, S. (2004). Growth increment patterns in the roots of two alpine forbs growing in the center and at the periphery of a snowbank. *Arctic, Antarctic, and Alpine Research*, 36(4), 591–597. [https://doi.org/10.1657/1523-0430\(2004\)036\[0591:GIPITR\]2.0.CO;2](https://doi.org/10.1657/1523-0430(2004)036[0591:GIPITR]2.0.CO;2)

EEA - European Environment Agency (2007) EU Habitats Directive Annex I: natural habitat types of community interest whose conservation requires the designation of special areas of conservation. European Council, Copenhagen, Denmark. Retrieved February 3, 2022 from eunis.eea.europa.eu/habitats/10084

EEA - European Environment Agency (2019) Heathlands, shrubs and sparsely vegetated lands. European Council, Copenhagen, Denmark. Retrieved February 3, 2022 from biodiversity.europa.eu/ecosystems/heathlands-shrubs-and-sparsely-vegetated-lands

Fonti, P., von Arx, G., García-González, I., Eilmann, B., Sass-Klaassen, U., Gärtner, H., & Eckstein, D. (2010). Studying global change through investigation of the plastic responses of xylem anatomy in tree rings. *New Phytologist*, 185(1), 42–53. <https://doi.org/10.1111/j.1469-8137.2009.03030.x>

Ganthaler, A., & Mayr, S. (2021). Subalpine dwarf shrubs differ in vulnerability to xylem cavitation: An innovative staining approach enables new insights. *Physiologia Plantarum*, 172(4), 2011–2021. <https://doi.org/10.1111/ppl.13429>

Gazol, A., & Camarero, J. J. (2012). Mediterranean dwarf shrubs and coexisting trees present different radial-growth synchronies and responses to climate. *Plant Ecology*, 213(10), 1687–1698. <https://doi.org/10.1007/s11258-012-0124-3>

Giménez-Benavides, L., Escudero, A., García-Camacho, R., García-Fernández, A., Iriondo, J. M., Lara-Romero, C., & Morente-López, J. (2018). How does climate change affect regeneration of Mediterranean high-mountain plants? An integration and synthesis of current knowledge. In *Plant Biology* (Vol. 20, pp. 50–62). Blackwell Publishing Ltd. <https://doi.org/10.1111/plb.12643>

Gimingham, C. H. (1972). Vegetational dynamics in *Calluna* heaths. *Verhandlungen - Gesellschaft Fur Okologie*, 25, 235–240.

Grant, S. A., & Hunter, R. F. (1962). Ecotypic Differentiation of *Calluna Vulgaris* (L.) in Relation To Altitude. *New Phytologist*, 61(1), 44–55. <https://doi.org/10.1111/j.1469-8137.1962.tb06272.x>

Guibal F., Guiot J. (2021) Dendrochronology. In: Ramstein G., Landais A., Bouttes N., Sepulchre P., Govin A. (eds) Paleoclimatology. Frontiers in Earth Sciences. Springer, Cham. https://doi.org/10.1007/978-3-030-24982-3_8

Gülsoy, S. K. (2021) Effect of altitude on some wood properties: A review Chapter · December 2021 · Use of glyceline in pulp production from Scots pine chips. <https://www.researchgate.net/publication/357687064>

Hacker, J., Ladinig, U., Wagner, J., & Neuner, G. (2011). Inflorescences of alpine cushion plants freeze autonomously and may survive subzero temperatures by supercooling. *Plant Science*, *180*(1), 149–156. <https://doi.org/10.1016/j.plantsci.2010.07.013>

Hallinger, M., Manthey, M., & Wilmking, M. (2010). Establishing a missing link: warm summers and winter snow cover promote shrub expansion into alpine tundra in Scandinavia. *New Phytologist*, *186*(4), 890–899. <https://doi.org/10.1111/j.1469-8137.2010.03223.x>

Ibe, K., Walmsley, D., Fichtner, A., Coners, H., Leuschner, C., & Härdtle, W. (2020). Provenance- and life-history stage-specific responses of the dwarf shrub *Calluna vulgaris* to elevated vapour pressure deficit. *Plant Ecology*, *221*(12), 1219–1232. <https://doi.org/10.1007/s11258-020-01076-3>

J. J (2020). “New features in the dendroTools R package: Bootstrapped and partial correlation coefficients for monthly and daily climate data.” *Dendrochronologia*, **63**, 125753. [doi:10.1016/j.dendro.2020.125753](https://doi.org/10.1016/j.dendro.2020.125753).

Jacobsen, A. L., Brandon Pratt, R., Venturas, M. D., & Hacke, U. G. (2019). Large volume vessels are vulnerable to water-stress-induced embolism in stems of poplar. *IAWA Journal*, *40*(1), 4–22. <https://doi.org/10.1163/22941932-40190233>

Jansen J (2002) Geobotanical guide of the Serra da Estrela. Lisbon: Institute for Nature Conservation, Ministry of Cities, Territorial Planning and Environment, 276 pp.

Jansen J (2005) De Serra da Estrela als referentiegebied voor herstel van heidelandschappen in de Lage Landen (with Englishsummary). DLN 106 (5): 186-189

Jansen, J. (2011). *Managing Natura 2000 in a changing world: The case of the Serra da Estrela (Portugal)*. BMC Public Health.

Jia, G., Shevliakova, E., Artaxo, P., de Noblet-Ducoudré, N., Houghton, R., Anderegg, W., Bernier, P., Carlo Espinoza, J., Semenov, S., Xu, X., Shevliakova, E., Artaxo, P., de Noblet-Ducoudré, N., Houghton, R., House, J., Kitajima, K., Lennard, C., Popp, A., Sirin, A., ... Malley, J. (2018). *Land-climate interactions - IPCC special report on climate change, desertification, land degradation, sustainable land management, food security, and greenhouse gas fluxes in terrestrial ecosystems*.

Kiaei, M., Moosavi, V., & Ebadi, S. E. (2019). Effects of altitude on density and biometric properties of hornbeam wood (*Carpinus betulus*). *Forest Systems*, 28(2). <https://doi.org/10.5424/fs/2019282-14490>

Körner, C. (2003) *Alpine plant life: functional plant ecology of high mountain ecosystems*. Berlin/Heidelberg: Springer Verlag. 978-3-642-18970-8. <https://doi.org/10.1007/978-3-642-18970-8>

Kuprian, E., Tuong, T. D., Pfaller, K., Wagner, J., Livingston, D. P., & Neuner, G. (2016). Persistent supercooling of reproductive shoots is enabled by structural ice barriers being active despite an intact xylem connection. *PLoS ONE*, 11(9). <https://doi.org/10.1371/journal.pone.0163160>

Lacerda R., Danielle. (2020) Assessing alpine shrub response to climate change. Ph.D. diss., University of Coimbra. <http://hdl.handle.net/10316/92203>

Lindholm, Mattias. (2019). *Heathlands – A Lost World?*

Malanson, G. P., Resler, L. M., Butler, D. R., & Fagre, D. B. (2019). Mountain plant communities: Uncertain sentinels? *Progress in Physical Geography*, 43(4), 521–543. <https://doi.org/10.1177/0309133319843873>

Mao, L., Chen, S., Zhang, J., & Zhou, G. (2016). Altitudinal patterns of maximum plant height on the Tibetan Plateau. *Journal of Plant Ecology*, 11(1), rtw128. <https://doi.org/10.1093/jpe/rtw128>

Martinez, L.H. (2005). Post Industrial Revolution human activity and climate change: Why the United States must implement mandatory limits on industrial Greenhouse Gas emissions. *Journal of Land Use and Environmental Law* 20(2): 403-421.

Meteoblue (2022, May 30) Arquivo meteorológico Serra da Estrela. www.meteoblue.com/pt/tempo/historyclimate/weatherarchive/serra-da-estrela_portugal_2739807.

Meyer-Grünefeldt, M., Belz, K., Calvo, L., Marcos, E., von Oheimb, G., & Härdtle, W. (2016). Marginal Calluna populations are more resistant to climate change, but not under high-nitrogen loads. *Plant Ecology*, 217(1), 111–122. <https://doi.org/10.1007/s11258-015-0563-8>

Moles, A. T., Warton, D. I., Warman, L., Swenson, N. G., Laffan, S. W., Zanne, A. E., Pitman, A., Hemmings, F. A., & Leishman, M. R. (2009). Global patterns in plant height. *Journal of Ecology*, 97(5), 923–932. <https://doi.org/10.1111/j.1365-2745.2009.01526.x>

Monschein, M., Iglesias Neira, J., Kunert, O., & Bucar, F. (2010). Phytochemistry of heather (*Calluna vulgaris* (L.) Hull) and its altitudinal alteration. *Phytochemistry Reviews*, 9(2), 205–215. <https://doi.org/10.1007/s11101-009-9153-5>.

Peguero-Pina, J. J., Vilagrosa, A., Alonso-Forn, D., Ferrio, J. P., Sancho-Knapik, D., & Gil-Pelegrín, E. (2020). Living in drylands: Functional adaptations of trees and shrubs to cope with high temperatures and water scarcity. In *Forests* (Vol. 11, Issue 10). MDPI AG. <https://doi.org/10.3390/F11101028>

Pereira, S. C., Carvalho, D., & Rocha, A. (2021). Temperature and precipitation extremes over the iberian peninsula under climate change scenarios: A review. In *Climate* (Vol. 9, Issue 9). MDPI. <https://doi.org/10.3390/cli9090139>.

- Piermattei, A., von Arx, G., Avanzi, C., Fonti, P., Gärtner, H., Piotti, A., Urbinati, C., Vendramin, G. G., Büntgen, U., & Crivellaro, A. (2020). Functional Relationships of Wood Anatomical Traits in Norway Spruce. *Frontiers in Plant Science*, 11. <https://doi.org/10.3389/fpls.2020.00683>
- Pisani, B., Samper, J., & Marques, J. E. (2019). Climate change impact on groundwater resources of a hard rock mountain region (Serra da Estrela, Central Portugal). *Sustainable Water Resources Management*, 5(1), 289–304. <https://doi.org/10.1007/s40899-017-0129-0>.
- Pittermann, J., & Sperry, J. S. (2006). Analysis of freeze-thaw embolism in conifers. The interaction between cavitation pressure and tracheid size. *Plant Physiology*, 140(1), 374–382. <https://doi.org/10.1104/pp.105.067900>
- Pugnaire, F. I., Losapio, G., & Schöb, C. (2021). Species interactions involving cushion plants in high-elevation environments under a changing climate. *Ecosistemas*, 30(1). <https://doi.org/10.7818/ECOS.2186>
- R Core Team (2020). R: A language and environment for statistical computing. R Foundation for Statistical Computing, Vienna, Austria. URL <https://www.R-project.org/>.
- Rahman, M.H., Kudo, K., Yamagishi, Y. *et al.* Winter-spring temperature pattern is closely related to the onset of cambial reactivation in stems of the evergreen conifer *Chamaecyparis pisifera*. *Sci Rep* 10, 14341 (2020). <https://doi.org/10.1038/s41598-020-70356-9>
- Rathgeber CBK, Cuny HE and Fonti P (2016) Biological Basis of Tree-Ring Formation: A Crash Course. *Front. Plant Sci.* 7:734. <https://doi.org/10.3389/fpls.2016.00734>
- Ren, P., Ziaco, E., Rossi, S., Biondi, F., Prislán, P., & Liang, E. (2019). Growth rate rather than growing season length determines wood biomass in dry environments. *Agricultural and Forest Meteorology*, 271, 46–53. <https://doi.org/10.1016/j.agrformet.2019.02.031>
- Ricker, M., Gutiérrez-García, G., Juárez-Guerrero, D., & Evans, M. E. K. (2020). Statistical age determination of tree rings. *PLoS ONE*, 15(9 September). <https://doi.org/10.1371/journal.pone.0239052>

Rieger, G., Müller, M., Guttenberger, H., & Bucar, F. (2008). Influence of altitudinal variation on the content of phenolic compounds in wild populations of *Calluna vulgaris*, *Sambucus nigra*, and *Vaccinium myrtillus*. *Journal of Agricultural and Food Chemistry*, 56(19), 9080–9086. <https://doi.org/10.1021/jf801104e>

Rivas-martínez, S., Rivas Sáenz, S., Penas, A., Alcaraz, F., Amigo, J., Asensi, A., Barbour, M., Biondi, E., Cantó, P., Capelo, J., Costa, J., Costa, M., del Arco, M., del Río, S., Díaz, T., Díez Garretas, B., Fernández-González, F., Gavilán, R., Gehú, J., ... Wildpret, W. (2011). Worldwide bioclimatic classification system. *Global Geobotany*, 1–634. <https://doi.org/10.5616/gg>

Román-Palacios, C., & Wiens, J. J. (2020). Recent responses to climate change reveal the drivers of species extinction and survival. *PNAS*, 117(8), 4211–4217. <https://doi.org/10.5061/dryad.4tmpg4f5w>

Schweingruber, F. H. (2007) *Wood Structure and Environment*. Springer Series in Wood Science. Springer 279p

Schweingruber, F. H., & Poschlod, P. (2005). *Forest Snow and Landscape Research Growth Rings in Herbs and Shrubs: life span, age determination and stem anatomy*. 79(3), 195–415.

Skendžić, S., Zovko, M., Živković, I. P., Lešić, V., & Lemić, D. (2021). Effect of climate change on introduced and native agricultural invasive insect pests in Europe. In *Insects* (Vol. 12, Issue 11). MDPI. <https://doi.org/10.3390/insects12110985>

Strona, G., & Bradshaw, C. J. A. (2018). Co-extinctions annihilate planetary life during extreme environmental change. *Scientific Reports*, 8(1). <https://doi.org/10.1038/s41598-018-35068-1>

Trexler, Adam. (2015). *Anthropocene Fictions: The Novel in a Time of Climate Change*. Charlottesville: University of Virginia Press.

Vieira, G., & Jansen, J. (2014). *Environmental setting of the Serra da Estrela, Portugal: a short-note ANTERMON | ANTArctic Electrical Resistivity Monitoring Network View project Aspiring Geopark Estrela View project*. <https://www.researchgate.net/publication/236323638>

Wang, H., Liu, H., Cao, G., Ma, Z., Li, Y., Zhang, F., Zhao, X., Zhao, X., Jiang, L., Sanders, N. J., Classen, A. T., & He, J. S. (2020). Alpine grassland plants grow earlier and faster but biomass remains unchanged over 35 years of climate change. In *Ecology Letters* (Vol. 23, Issue 4, pp. 701–710). Blackwell Publishing Ltd. <https://doi.org/10.1111/ele.13474>

Weijers, S., Greve Alsos, I., Bronken Eidesen, P., Broekman, R., Loonen, M. J. J. E., & Rozema, J. (2012). No divergence in *Cassiope tetragona*: persistence of growth response along a latitudinal temperature gradient and under multi-year experimental warming. *Annals of Botany*, 110(3), 653–665. <https://doi.org/10.1093/aob/mcs123>

Winkler, D. E., Lubetkin, K. C., Carrell, A. A., Jabis, M. D., Yang, Y., & Kueppers, L. M. (2019). Responses of alpine plant communities to climate warming. In *Ecosystem Consequences of Soil Warming: Microbes, Vegetation, Fauna and Soil Biogeochemistry* (pp. 297–346). Elsevier. <https://doi.org/10.1016/B978-0-12-813493-1.00013-2>

Yang, D., Wang, A.-Y., Zhang, J.-L., Bradshaw, C. J. A., & Hao, G.-Y. (2020). Variation in Stem Xylem Traits is Related to Differentiation of Upper Limits of Tree Species along an Elevational Gradient. *Forests*, 11(3), 349. <https://doi.org/10.3390/f11030349>.

Weiner, J. (2004). Allocation, plasticity and allometry in plants. *Perspectives in Plant Ecology, Evolution and Systematics*, 6(4), 207–215. <https://doi.org/10.1078/1433-8319-00083>

Walter, J., Harter, D. E. V., Beierkuhnlein, C., & Jentsch, A. (2016). Transgenerational effects of extreme weather: perennial plant offspring show modified germination, growth and stoichiometry. *Journal of Ecology*, 104(4), 1032–1040. <https://doi.org/10.1111/1365-2745.12567>

Appendix

Appendix 1 - List of species protected by Natura 2000

Natura 2000	Species scientific name	English common name	Species group ▼
1172	<i>Chioglossa lusitanica</i>	Gold-striped salamander	Amphibians
1194	<i>Discoglossus galganoi</i>	Iberian painted frog	Amphibians
1116	<i>Chondrostoma polylepis</i>	Iberian nase	Fishes
5302	<i>Cobitis paludica</i>		Fishes
1135	<i>Rutilus macrolepidotus</i>	Ruivaco	Fishes
1793	<i>Centaurea micrantha</i> subsp. <i>herminii</i>		Flowering Plants
1784	<i>Centaurea rothmalerana</i>		Flowering Plants
1885	<i>Festuca elegans</i>		Flowering Plants
1890	<i>Festuca henriquesii</i>		Flowering Plants
1891	<i>Festuca summilusitana</i>		Flowering Plants
1865	<i>Narcissus asturiensis</i>		Flowering Plants
1857	<i>Narcissus pseudonarcissus</i> subsp. <i>nobilis</i>		Flowering Plants
1733	<i>Veronica micrantha</i>		Flowering Plants
1078	<i>Callimorpha quadripunctaria</i>	Jersey Tiger	Invertebrates

1044	<i>Coenagrion mercuriale</i>	Southern Coenagrion	Invertebrates
1065	<i>Euphydryas aurinia</i>	Marsh Fritillary	Invertebrates
1024	<i>Geomalacus maculosus</i>	Kerry Slug	Invertebrates
1046	<i>Gomphus graslinii</i>		Invertebrates
1083	<i>Lucanus cervus</i>	Stag Beetle	Invertebrates
1036	<i>Macromia splendens</i>	Shining Macromia	Invertebrates
1041	<i>Oxygastra curtisii</i>	Orange-spotted Emerald	Invertebrates
1308	<i>Barbastella barbastellus</i>	Barbastelle	Mammals
1301	<i>Galemys pyrenaicus</i>	Pyrenean desman	Mammals
1355	<i>Lutra lutra</i>	Eurasian otter	Mammals
1310	<i>Miniopterus schreibersii</i>	Schreiber's Bat	Mammals
1323	<i>Myotis bechsteinii</i>	Bechstein's bat	Mammals
1307	<i>Myotis blythii</i>	Lesser mouse-eared bat	Mammals
1321	<i>Myotis emarginatus</i>	Geoffroy's bat	Mammals
1324	<i>Myotis myotis</i>	Greater mouse-eared bat	Mammals
1305	<i>Rhinolophus euryale</i>	Mediterranean horseshoe bat	Mammals
1304	<i>Rhinolophus ferrumequinum</i>	Greater horseshoe bat	Mammals
1303	<i>Rhinolophus hipposideros</i>	Lesser horseshoe bat	Mammals
1304	<i>Rhinolophus ferrumequinum</i>	Greater horseshoe bat	Mammals
1303	<i>Rhinolophus hipposideros</i>	Lesser horseshoe bat	Mammals
1385	<i>Bruchia vogesiaca</i>		Mosses & Liverworts
1390	<i>Marsupella profunda</i>		Mosses & Liverworts
1249	<i>Lacerta monticola</i>	Iberian rock lizard	Reptiles
1259	<i>Lacerta schreiberi</i>	Schreiber's green lizard	Reptiles
1221	<i>Mauremys leprosa</i>	Spanish terrapin	Reptiles

Appendix 2 - List of habitat types protected by Natura 2000

Habitat type code	Habitat type english name
3130	Oligotrophic to mesotrophic standing waters with vegetation of the Littorelletea uniflorae and/or of the Isoeto-Nanojuncetea
3170	Mediterranean temporary ponds
3260	Water courses of plain to montane levels with the Ranunculion fluitantis and Callitriche-Batrachion vegetation
3290	Intermittently flowing Mediterranean rivers of the Paspalo-Agrostidion
4010	Northern Atlantic wet heaths with Erica tetralix
4020	Temperate Atlantic wet heaths with Erica ciliaris and Erica tetralix
4030	European dry heaths
4060	Alpine and Boreal heaths
4090	Endemic oro-Mediterranean heaths with gorse
5120	Mountain Cytisus purgans formations
5230	Arborescent matorral with Laurus nobilis
6160	Oro-Iberian Festuca indigesta grasslands
6230	Species-rich Nardus grasslands, on siliceous substrates in mountain areas (and submountain areas in Continental Europe)
6410	Molinia meadows on calcareous, peaty or clayey-silt-laden soils (Molinion caeruleae)
6430	Hydrophilous tall herb fringe communities of plains and of the montane to alpine levels
6510	Lowland hay meadows (Alopecurus pratensis, Sanguisorba officinalis)
7140	Transition mires and quaking bogs
8130	Western Mediterranean and thermophilous scree
8220	Siliceous rocky slopes with chasmophytic vegetation
8230	Siliceous rock with pioneer vegetation of the Sedo-Scleranthion or of the Sedo albi-Veronicion dillenii
8310	Caves not open to the public
91B0	Thermophilous Fraxinus angustifolia woods
91E0	Alluvial forests with Alnus glutinosa and Fraxinus excelsior (Alno-Padion, Alnion incanae, Salicion albae)
9230	Galicio-Portuguese oak woods with Quercus robur and Quercus pyrenaica
9260	Castanea sativa woods
92A0	Salix alba and Populus alba galleries
92D0	Southern riparian galleries and thickets (Nerio-Tamaricetea and Securinegion tinctoriae)
9330	Quercus suber forests
9340	Quercus ilex and Quercus rotundifolia forests
9380	Forests of Ilex aquifolium
9580	Mediterranean Taxus baccata woods

Appendix 3 - Field sheet example

Ficha de campo

Data: 21/09/2021

Autores presentes: Cristina Nabais, Marta e Susana

Local: Covão dos conchos (BUR)

Concelho/Distrito: Seia/ Guarda

Declive: Plano

Exposição solar: Total

Altitude: 1630 metros

Código	Altura (cm)	Diâmetro (cm)	Distância next (cm)	GPS (Este/Oeste; Norte)
BUR1	42	140*122	60	40.364482 -7.609568
BUR2	50	107*103	170	
BUR3	42	130*100	60	
BUR4	44	100*87	120	
BUR5	28	134*109	30	
BUR6	51	156*93	0	

Outras espécies
<u>Juniperus</u>
<u>Cytisus striatus</u>
<u>Halimium umbellatum</u>
Erica

*Floração maioritariamente fechada (rosa)

Appendix 4 - Not-shrub species recorded while sampling

<i>Mid and High belt</i>	<i>Low belt</i>
<i>Armeria beirana</i>	<i>Baccharis trimera</i>
<i>Carex furva</i>	<i>Eucalyptus globulus Labill</i>
<i>Halimium umbellatum</i>	<i>Pinus sylvestris</i>
<i>Juncus squarrosus</i>	
<i>Nardus stricta</i>	

Appendix 5 – Table of mean climatic characteristics at the sampling sites of C. vulgaris individuals. Data was gathered from TerraClimate 2020 source and divided by elevation.

<i>Year</i>	<i>Max Temperature</i>			<i>Min Temperature</i>			<i>Precipitation</i>		
	<i>High</i>	<i>Mid</i>	<i>Low</i>	<i>High</i>	<i>Mid</i>	<i>Low</i>	<i>High</i>	<i>Mid</i>	<i>Low</i>
2000	11.60	11.48	20.21	4.64	4.52	10.62	1990.8	1998.1	1103.0
2001	11.49	11.38	20.08	4.83	4.71	10.77	1894.1	1900.3	1181.1
2002	11.24	11.13	19.83	4.67	4.55	10.60	1980.9	1989.6	1158.2
2003	11.96	11.84	20.57	5.27	5.16	11.23	2078.8	2085.8	1221.6
2004	11.76	11.64	20.42	4.63	4.51	10.60	1422.6	1425.8	847.1
2005	12.13	12.01	20.76	4.32	4.21	10.30	1168.3	1172.6	669.1
2006	12.28	12.17	20.88	5.41	5.30	11.38	2049.8	2056.8	1238.3
2007	11.46	11.34	20.06	4.63	4.52	10.64	1430.5	1435.8	839.5
2008	11.32	11.21	19.92	4.83	4.71	10.85	1664.0	1668.1	1026.8
2009	12.20	12.08	20.74	5.37	5.25	11.34	1803.9	1809.9	1117.0
2010	11.68	11.56	20.35	4.72	4.61	10.67	2729.5	2735.1	1698.1
2011	12.41	12.29	21.04	4.95	4.83	10.90	1710.8	1714.4	1093.9
2012	12.28	12.16	21.02	4.37	4.25	10.23	1459.6	1462.6	917.0
2013	12.12	12.00	20.86	4.29	4.18	10.12	2044.5	2049.9	1264.9
2014	12.75	12.64	21.46	4.56	4.44	10.35	2032.9	2039.6	1283.0
2015	13.11	12.99	21.84	4.25	4.14	10.08	1150.2	1154.1	678.6
2016	12.57	12.45	21.33	4.56	4.44	10.42	2055.3	2061.6	1193.5
2017	13.32	13.21	22.06	4.62	4.51	10.48	1203.5	1208.9	737.8
2018	12.29	12.17	21.04	4.46	4.35	10.31	2072.5	2080.5	1212.9
2019	12.04	11.92	20.50	5.01	4.89	10.68	1500.8	1510.6	916.0
2020	12.68	12.56	21.05	5.71	5.60	11.37	1525.6	1527.8	905.9

Appendix 6 – Table of Pearson’s correlation between individuals in Low elevation (CAR, MIS, and IPA). Highlights on positive correlations.

	CAR1	CAR2	CAR4	CAR5	IPA2	IPA3	IPA4	IPA6	MIS1	MIS2	MIS3
CAR1	1.000										
CAR2	0.572	1.000									
CAR4	0.805	0.744	1.000								
CAR5	0.684	0.664	0.860	1.000							
IPA2	0.928	0.320	0.228	0.228	1.000						
IPA3	0.568	0.516	0.257	0.257	0.797	1.000					
IPA4	0.391	0.829	0.422	0.422	0.425	0.850	1.000				
IPA6	-0.121	-0.307	-0.088	-0.396	0.880	0.588	0.268	1.000			
MIS1	-0.136	-0.359	-0.461	-0.329	0.263	-0.400	-0.559	-0.382	1.000		
MIS2	-0.835	-0.766	-0.664	-0.482	-0.673	-0.849	-0.872	-0.061	0.356	1.000	
MIS3	0.247	-0.157	0.128	-0.320	-0.046	-0.606	-0.732	-0.431	-0.114	0.298	1.000

Appendix 7- Table of Pearson's correlation between individuals in Mid (CAM, BUR, and LAC) and High elevation (COV, CUM, and ALX).

Highlights on positive correlations.

	BUR2	BUR3	BUR4	CAM2	CAM4	LAC2	LAC3	LAC5	LAC6	ALX1	ALX2	ALX3	ALX5	COV1	COV2	COV3	COV4	COV5	COV6	CUM1	CUM2	CUM3	CUM4	CUM5	
BUR2	1.000																								
BUR3	0.319	1.000																							
BUR4	0.630	0.376	1.000																						
CAM2	0.367	-0.278	0.383	1.000																					
CAM4	-0.493	-0.210	-0.514	0.434	1.000																				
LAC2	0.251	0.280	0.283	-0.295	-0.512	1.000																			
LAC3	0.414	0.432	0.522	0.077	-0.397	0.713	1.000																		
LAC5	0.458	0.718	0.117	-0.201	-0.288	0.481	0.230	1.000																	
LAC6	0.661	0.034	0.259	0.577	0.143	-0.088	0.223	0.274	1.000																
ALX1	0.238	0.128	0.141	0.480	0.404	-0.289	-0.126	-0.309	0.336	1.000															
ALX2	-0.083	0.507	-0.379	-0.141	0.201	-0.004	-0.067	0.355	-0.163	-0.218	1.000														
ALX3	0.247	0.376	0.654	0.333	-0.039	0.203	0.315	-0.087	-0.032	0.567	-0.355	1.000													
ALX5	-0.309	0.426	-0.504	-0.268	0.322	0.148	-0.053	0.292	-0.332	-0.468	0.754	-0.453	1.000												
COV1	-0.057	0.857	-0.719	-0.239	0.009	0.094	0.229	0.396	-0.155	0.173	0.414	0.334	0.491	1.000											
COV2	0.196	0.490	-0.305	0.492	-0.120	0.216	0.229	0.552	0.081	0.093	0.547	-0.101	0.729	0.501	1.000										
COV3	0.289	0.323	0.199	-0.625	-0.544	0.698	0.365	0.222	-0.258	0.082	0.055	0.356	-0.063	-0.009	-0.138	1.000									
COV4	0.593	-0.030	0.790	0.320	-0.362	0.276	0.662	-0.152	0.311	-0.203	-0.265	0.148	-0.349	-0.456	-0.332	0.097	1.000								
COV5	0.518	0.290	0.833	-0.097	-0.342	0.264	0.232	-0.049	0.098	0.349	-0.438	0.576	-0.372	-0.099	-0.215	0.533	0.530	1.000							
COV6	0.390	-0.036	0.196	0.640	0.642	-0.387	-0.016	0.380	0.764	0.120	0.428	-0.185	0.013	-0.394	0.417	-0.620	0.069	-0.358	1.000						
CUM1	0.559	0.652	-0.596	-0.855	-0.583	0.572	0.431	0.799	0.408	-0.174	0.253	-0.786	0.092	0.158	0.138	0.801	-0.284	-0.449	0.112	1.000					
CUM2	0.399	0.138	0.154	0.301	0.313	0.259	-0.468	0.008	0.531	0.840	0.297	0.268	0.206	-0.534	0.959	0.525	-0.609	0.549	0.324	0.141	1.000				
CUM3	0.085	0.853	0.354	-0.625	-0.318	0.064	0.460	0.486	-0.213	-0.137	0.453	0.091	0.462	0.799	0.288	0.263	0.224	0.238	-0.513	0.725	-0.150	1.000			
CUM4	0.316	0.564	0.080	0.170	0.356	0.125	0.147	0.371	0.499	-0.017	0.584	-0.136	0.351	-0.205	0.342	0.341	0.397	0.393	0.272	-0.174	0.200	0.407	1.000		
CUM5	-0.175	0.178	-0.122	-0.564	-0.190	-0.069	-0.421	-0.039	-0.278	-0.044	0.118	-0.428	0.241	-0.290	-0.174	0.693	-0.016	0.370	-0.617	0.134	0.260	0.574	0.661	1.000	

Appendix 8 - Table with *Calluna vulgaris* individuals with location (GPS coordinates measured in the field), altitude, height, and shrub diameter. Data in bold in mean and standard error values.

<i>Elev</i>	<i>Local e concelho</i>	<i>Altitude (m)</i>	<i>Ind</i>	<i>Height (cm)</i>	<i>Diameter (cm)</i>	<i>GPS</i>
			COV1	30	230	40,32476, -7,60106
			COV2	26	120	40,32450, -7,60130
	COV – Covão do boí	1868	COV3	20	170	40,32397, -7,60205
	Manteigas		COV4	20	160	40,32389, -7,60235
			COV5	30	110	40,32376, -7,60263
			COV6	25	176	40,32379, -7,60277
			COV	25.17 ± 1.67	161 ± 16.12	
				CUM1	23	100
			CUM2	15	88	40,34700, -7,62336
High	CUM – Sabugueiro	1862	CUM3	35	130	40,34707, -7,62373
	Seia		CUM4	20	100	40,34708, -7,62397
			CUM5	27	80	40,34709, -7,62417
			CUM6	18	100	40,34718, -7,62465
			CUM	23.00 ± 2.68	99.67 ± 6.33	
				ALX1	32	123
			ALX2	30	88	40,340810, -7,639865
	ALX – Lorigã	1824	ALX3	46	120	40,340846, -7,640033
	Seia		ALX4	33	125	40,340924, -7,640137
			ALX5	25	110	40,340795, -7,640415
			ALX6	40	167	40,340701, -7,640653
			ALX	34.33 ± 2.80	122.17 ± 9.63	
				Mean	27.50 ± 1.82	127.61 ± 8.90
			CAM1	39	115	40.363654, -7.629947
			CAM2	34	90	40.363654, -7.629947
	CAM – A caminho do	1680	CAM3	50	91	40.363654, -7.629947
	BUR		CAM4	60	95	40.363654, -7.629947
	Seia		CAM5	70	100	40.363654, -7.629947
Mid			CAM6	61	90	40.363654, -7.629947
			CAM	52.33 ± 5.18	96.83 ± 3.62	
			1630	BUR1	42	140

<i>Elev</i>	<i>Local e concelho</i>	<i>Altitude (m)</i>	<i>Ind</i>	<i>Height (cm)</i>	<i>Diameter (cm)</i>	<i>GPS</i>
			BUR2	50	107	40.364482, -7.609568
	BUR – Covão dos conchos		BUR3	42	130	40.364482, -7.609568
	Seia		BUR4	44	100	40.364482, -7.609568
			BUR5	28	134	40.364482, -7.609568
			BUR6	51	156	40.364482, -7.609568
			BUR	42.83 ± 5.18	127.83 ± 5.18	
			LAC1	25	110	40.35984, -7.65294
	LAC – Lagoa comprida		LAC2	20	120	40.35992, -7.65286
	Seia	1598	LAC3	35	100	40.35998, -7.65284
			LAC4	30	110	40.36012, -7.65284
			LAC5	35	90	40.36020, -7.65298
			LAC6	30	110	40.36037, -7.65298
			LAC	29.17 ± 2.18	106.67 ± 3.85	
			Mean	41.44 ± 3.10	110.44 ± 4.38	
			CAR1	105	145	40.245228, -8.362795
	CAR – Carapinheira da Serra		CAR2	140	114	40.245228, -8.362795
	Coimbra	345	CAR3	110	90	40.245228, -8.362795
			CAR4	105	96	40.245228, -8.362795
			CAR5	89	82	40.245228, -8.362795
			CAR6	165	142	40.245228, -8.362795
			CAR	119.00 ± 10.45	111.50 ± 10.04	
Low	MIS – Misarela		MIS1	108	79	40.213487, -8.363134
	Montealegre	203	MIS2	115	60	40.213487, -8.363134
			MIS3	100	55	40.213487, -8.363134
			MIS4	58	40	40.213487, -8.363134
			MIS5	60	34	40.213487, -8.363134
			MIS6	70	35	40.213487, -8.363134
			MIS	85.17 ± 9.48	50.50 ± 6.55	
			IPA1	56	55	40.177902, -8.463636
	IPA – IPark Coimbra		IPA2	61	53	40.177902, -8.463636
	Coimbra	181	IPA3	58	53	40.177902, -8.463636
			IPA4	51	54	40.177902, -8.463636
			IPA5	59	39	40.177902, -8.463636

<i>Elev</i>	<i>Local e concelho</i>	<i>Altitude (m)</i>	<i>Ind</i>	<i>Height (cm)</i>	<i>Diameter (cm)</i>	<i>GPS</i>
			IPA6	65	37	40.177902, -8.463636
			IPA	58.33 ± 1.76	48.50 ± 3.05	
			Mean	87.50 ± 7.53	70.17 ± 8.03	

Appendix 9 - Table with *Calluna vulgaris* individuals' age, shrub-ring-width (SRW), average vessel area (AVA), and cell wall percentage (PCW). Characteristics calculated for the years 2016-2020. Mean individual age and other variables were calculated from the raw data (3 branches) of each individual. Data in mean SE (Standard Error).

<i>Elev</i>	<i>Ind</i>	<i>Age (years)</i>	<i>SRW (µm)</i>	<i>AVA (µm²)</i>	<i>Cell wall (%)</i>
	COV1	11.33 ± 1.78	133.11 ± 10.79	33.86 ± 2.03	57.32 ± 1.52
	COV2	11.00 ± 1.89	249.70 ± 18.76	47.51 ± 3.79	56.56 ± 1.37
	COV3	9.67 ± 1.19	348.25 ± 40.31	48.80 ± 4.00	51.95 ± 1.66
	COV4	8.67 ± 0.72	324.46 ± 25.50	46.24 ± 2.95	62.10 ± 2.61
	COV5	9.67 ± 0.98	186.27 ± 17.37	40.04 ± 2.49	67.74 ± 1.39
	COV6	8.00 ± 0.47	405.66 ± 24.22	44.97 ± 3.30	61.95 ± 1.71
	COV	9.72 ± 0.59	274.58 ± 14.14	43.57 ± 1.40	59.60 ± 0.89
	CUM1	5.33 ± 0.54	338.18 ± 42.97	33.47 ± 1.73	70.53 ± 1.08
	CUM2	4.67 ± 0.27	324.80 ± 28.67	24.30 ± 1.07	75.84 ± 0.40
	CUM3	18.67 ± 1.19	140.83 ± 16.46	45.51 ± 5.07	72.70 ± 0.82
	CUM4	7.00 ± 0.00	223.32 ± 24.01	29.32 ± 2.03	74.30 ± 0.84
	CUM5	7.00 ± 0.47	405.37 ± 33.24	42.49 ± 2.53	73.58 ± 1.35
	CUM6	14.00 ± 1.63	191.36 ± 29.39	32.78 ± 1.35	67.57 ± 1.03
	CUM	9.44 ± 1.26	269.26 ± 15.72	34.13 ± 1.26	72.39 ± 0.50
High	ALX1	10.67 ± 0.54	212.40 ± 30.09	46.22 ± 2.61	68.03 ± 1.37
	ALX2	13.00 ± 0.82	322.00 ± 33.25	47.13 ± 3.06	60.15 ± 0.65
	ALX3	10.33 ± 0.98	315.13 ± 45.26	36.34 ± 2.68	60.30 ± 1.40
	ALX4	13.67 ± 1.19	226.30 ± 32.59	45.48 ± 3.27	59.92 ± 0.81
	ALX5	11.33 ± 1.78	324.89 ± 28.24	48.92 ± 4.14	59.80 ± 2.51
	ALX6	22.00 ± 0.47	249.73 ± 24.15	39.46 ± 1.35	60.57 ± 1.25

	ALX	13.50 ± 1.03	275.07 ± 14.32	43.92 ± 1.30	61.46 ± 0.67
	Mean	10.89 ± 0.63	273.00 ± 32.83	40.71 ± 3.13	64.27 ± 2.06
Mid	CAM1	14.00 ± 0.82	419.11 ± 38.13	33.12 ± 1.55	67.91 ± 1.11
	CAM2	7.67 ± 1.09	371.88 ± 30.21	42.25 ± 1.59	64.09 ± 0.85
	CAM3	11.00 ± 0.47	283.03 ± 17.75	41.72 ± 1.08	63.77 ± 1.56
	CAM4	15.00 ± 1.25	290.94 ± 16.63	43.12 ± 1.67	63.66 ± 1.19
	CAM5	6.67 ± 0.27	338.36 ± 24.18	32.85 ± 1.59	66.62 ± 0.69
	CAM6	11.00 ± 0.47	217.67 ± 16.89	37.62 ± 1.62	65.92 ± 1.54
	CAM	10.89 ± 0.79	320.16 ± 12.39	38.45 ± 0.77	65.33 ± 0.52
	BUR1	14.33 ± 0.98	206.08 ± 25.38	39.32 ± 1.55	54.83 ± 1.67
	BUR2	12.00 ± 1.41	219.68 ± 39.16	23.35 ± 1.59	67.65 ± 1.12
	BUR3	15.33 ± 0.72	89.27 ± 8.96	37.87 ± 1.08	63.32 ± 1.32
	BUR4	7.67 ± 0.27	251.18 ± 20.58	33.86 ± 1.67	58.60 ± 1.11
	BUR5	15.67 ± 0.98	185.07 ± 16.77	45.51 ± 1.59	58.24 ± 2.32
	BUR6	12.67 ± 1.66	267.65 ± 24.96	34.47 ± 1.62	64.27 ± 1.40
	BUR	13.00 ± 0.80	202.18 ± 11.25	36.46 ± 1.02	60.77 ± 0.79
	LAC1	13.00 ± 2.36	222.49 ± 36.56	42.43 ± 1.74	68.41 ± 1.75
	LAC2	21.33 ± 1.78	212.59 ± 21.83	41.64 ± 2.83	61.69 ± 1.05
	LAC3	10.67 ± 1.09	199.48 ± 25.53	34.63 ± 1.42	69.44 ± 1.21
	LAC4	15.00 ± 0.00	244.01 ± 18.10	42.57 ± 4.97	67.38 ± 3.20
	LAC5	9.67 ± 0.72	236.93 ± 29.67	40.06 ± 2.68	67.29 ± 1.64
	LAC6	11.33 ± 1.53	337.03 ± 22.72	38.00 ± 2.53	63.52 ± 1.44
	LAC	13.41 ± 1.16	241.97 ± 12.24	39.73 ± 1.13	66.22 ± 0.75
Mean	12.40 ± 0.56	256.03 ± 28.78	38.22 ± 2.16	64.13 ± 1.61	
	CAR1	5.67 ± 0.27	592.70 ± 90.90	32.09 ± 2.05	72.64 ± 1.25
	CAR2	5.50 ± 0.35	408.26 ± 55.62	40.75 ± 2.06	70.54 ± 0.79
	CAR3	8.33 ± 0.54	357.21 ± 57.59	45.57 ± 2.75	61.37 ± 2.70
	CAR4	5.67 ± 0.54	483.07 ± 67.02	38.76 ± 2.75	69.14 ± 1.95
	CAR5	8.33 ± 0.72	447.25 ± 71.60	35.53 ± 2.04	69.15 ± 1.26
	CAR6	3.67 ± 0.27	660.74 ± 124.64	52.73 ± 5.66	55.24 ± 5.27

	CAR	6.24 ± 0.46	488.32 ± 34.47	40.33 ± 1.41	66.63 ± 1.19
	MIS1	8.00 ± 0.47	272.49 ± 80.41	36.89 ± 2.53	66.57 ± 1.25
	MIS2	9.33 ± 0.27	289.84 ± 52.40	28.62 ± 1.87	70.22 ± 1.35
	MIS3	6.67 ± 1.78	257.86 ± 37.91	36.62 ± 1.65	63.15 ± 3.15
	MIS4	4.00 ± 0.71	312.90 ± 68.60	27.74 ± 1.79	68.92 ± 2.01
Low	MIS5	5.33 ± 0.27	534.22 ± 87.81	28.08 ± 1.47	70.31 ± 1.18
	MIS6	4.50 ± 0.35	411.24 ± 92.84	24.21 ± 1.53	74.51 ± 1.20
	MIS	6.56 ± 0.59	345.56 ± 31.97	31.01 ± 0.96	68.59 ± 0.86
	IPA1	5.00 ± 0.00	387.16 ± 45.06	46.81 ± 3.95	67.40 ± 1.40
	IPA2	6.00 ± 1.41	432.01 ± 30.80	59.00 ± 5.51	71.87 ± 2.20
	IPA3	4.67 ± 0.27	550.48 ± 67.41	39.21 ± 2.49	71.09 ± 0.96
	IPA4	4.67 ± 0.27	498.38 ± 71.15	39.17 ± 2.47	73.81 ± 1.36
	IPA5	4.50 ± 0.35	377.86 ± 89.39	48.00 ± 13.67	78.91 ± 0.94
	IPA6	4.00 ± 0.94	463.97 ± 129.58	49.42 ± 2.47	68.11 ± 2.12
	IPA	4.75 ± 0.30	456.72 ± 32.42	45.92 ± 2.30	71.47 ± 0.76
	Mean	5.86 ± 0.29	431.01 ± 69.69	38.99 ± 3.63	68.80 ± 2.06

Appendix 10 - Results of LMER function in R for residuals and correlation of fixed effects for the altitude in the SRW model.

Linear mixed model fit by REML. t-tests use Satterthwaite's method [`lmerModLmerTest`]
 Formula: `Residuals ~ Alt_avg + (1 | Ano) + (1 | Altitude)`
 Data: `Table_TRW_per_plant`

REML criterion at convergence: -133.8

Scaled residuals:

Min	1Q	Median	3Q	Max
-4.7285	-0.5553	0.1265	0.6500	2.9341

Random effects:

Groups	Name	Variance	Std.Dev.
Altitude	(Intercept)	0.004483	0.06695
Ano	(Intercept)	0.001447	0.03804
	Residual	0.030248	0.17392

Number of obs: 267, groups: Altitude, 9; Ano, 5

Fixed effects:

	Estimate	Std. Error	df	t value	Pr(> t)
(Intercept)	5.367e-02	5.265e-02	8.445e+00	1.019	0.336
Alt_avg	-4.295e-05	3.474e-05	7.045e+00	-1.236	0.256

Correlation of Fixed Effects:

	(Intr)
Alt_avg	-0.822

Appendix 11 – Results of LMER function in R for residuals and correlation of fixed effects for the altitude in the AVA model.

Linear mixed model fit by REML [`lmerMod`]
 Formula: `AVG_AVA ~ Elev + (1 | Ano) + (1 | Local)`
 Data: `Data1`

REML criterion at convergence: 545.8

Scaled residuals:

Min	1Q	Median	3Q	Max
-4.8149	-0.5863	-0.0320	0.6675	3.1754

Random effects:

Groups	Name	Variance	Std.Dev.
Local	(Intercept)	0.17743	0.4212
Ano	(Intercept)	0.02389	0.1546
	Residual	0.39915	0.6318

Number of obs: 269, groups: Local, 9; Ano, 5

Fixed effects:

	Estimate	Std. Error	t value
(Intercept)	6.3464	0.2615	24.274
ElevLow	-0.1905	0.3567	-0.534
ElevMid	-0.2013	0.3566	-0.565

Correlation of Fixed Effects:

	(Intr)	ElevLw
ElevLow	-0.682	
ElevMid	-0.682	0.500

Appendix 12 – Results of LMER function in R for residuals and correlation of fixed effects for the altitude in the PCW model.

```
Linear mixed model fit by REML ['lmerMod']  
Formula: AVG_PCellWall ~ Elev + (1 | Ano) + (1 | Local)  
Data: Data1
```

REML criterion at convergence: 1607.6

Scaled residuals:

Min	1Q	Median	3Q	Max
-3.3629	-0.5306	0.0041	0.6709	2.2169

Random effects:

Groups	Name	Variance	Std.Dev.
Local	(Intercept)	20.1071	4.4841
Ano	(Intercept)	0.2569	0.5068
Residual		21.5760	4.6450

Number of obs: 269, groups: Local, 9; Ano, 5

Fixed effects:

	Estimate	Std. Error	t value
(Intercept)	64.4947	2.6445	24.388
ElevLow	4.7089	3.7265	1.264
ElevMid	-0.2384	3.7261	-0.064

Correlation of Fixed Effects:

	(Intr)	ElevLw
ElevLow	-0.704	
ElevMid	-0.705	0.500